RESEARCH IN SUPPORT OF THE EODAP VALIDATION PROGRAM

AND

SOLID EARTH GEOPHYSICS

Grant NSG 5148

Final Report

1 December 1976 to 30 September 1977

Principal Investigator

Dr. E. M. Gaposchkin

Prepared for

National Aeronautics and Space Administration
Greenbelt, Maryland 20771

September 1978

Smithsonian Institution
Astrophysical Observatory
Cambridge, Massachusetts 02138

The Smithsonian Astrophysical Observatory
and the Harvard College Observatory
are members of the
Center for Astrophysics

RESEARCH IN SUPPORT OF THE EODAP VALIDATION PROGRAM

AND

SOLID EARTH GEOPHYSICS

Grant NSG 5148

Final Report

1 December 1976 to 30 September 1977

Principal Investigator

Dr. E. M. Gaposchkin

Prepared for

National Aeronautics and Space Administration
Greenbelt, Maryland 20771

September 1978

Smithsonian Institution
Astrophysical Observatory
Cambridge, Massachusetts 02138

TABLE OF CONTENTS

RESEARCH IN SUPPORT OF THE EODAP VALIDATION PROGRAM
AND
SOLID EARTH GEOPHYSICS

FINAL REPORT

1. INTRODUCTION

The Smithsonian Astrophysical Observatory (SAO) program of participation in the Earth and Ocean Dynamics Application Program (EODAP) of the National Aeronautics and Space Administration (NASA) has been directed toward many of the EODAP objectives. As one element of this participation, the analysis program reported here, has concentrated on the validation program — that is, to verify that geodetic space techniques can measure intersite distances of several hundred to several thousand kilometers and polar motion, both with a precision of about 5 cm.

The original scope of this program element was intended to be broad, examining several options for acquiring and analyzing satellite laser data, and planning and executing an observation program and the final data analysis to obtain a geophysical measurement. This program was envisioned to be a multi-year effort, proceeding through development of an operational system to support a primary EODAP objective - viz., the definition of Earthquake Hazard Assessment Models. Because of NASA's decision to redirect EODAP program resources, and the notification that no follow-on work would be supported in this area, SAO has phased out its capability in analysis of laser data, and charged the associated termination costs to this grant. Therefore the level of effort applied to this analysis, and the results are less ambitious than originally envisioned. The effort has almost totally been devoted to analysis of laser data using a new analytical approach "Scalar Translocation." Based on a limited but diverse set of data, it was found that this approach can give geodynamic information and that the method is promising and can be used on a variety of satellites with data of different accuracy. This rescoping of the effort was negotiated with contract monitor, Dr. David Smith (NASA, Greenbelt).

2. TECHNICAL APPROACH

"Scalar Translocation" is a method of analyzing satellite laser range data for accurately determining interstation baselines. It uses short (less than one revolution) overlapping arcs of laser data, from two stations to determine interstation distance. This distance is relatively uncorrupted by satellite orbital errors, is independent of satellite orbit scale, and, with suitable data distribution, is independent of range bias and noise in the data. With this technique, a number of baseline determinations could be averaged to provide an optimum estimate of the baseline, or could be analyzed as a time series to measure the periodic horizontal tidal displacement (the love number l) or the secular displacement. A network of such baselines could be adjusted or combined with other types of data to obtain station coordinates.

The basic theory of "Scalar Translocation" has been given in Latimer and Gaposchkin (1977) with some results. That report is included as Appendix A, and will be used as the basic theoretical framework for the results given here.

The additional data analysis has taken a number of consecutive steps. As described in Latimer and Gaposchkin, a number of data sets are available from previous observing programs. Though none of these programs (1967-DIADEM, 1968-RCP133/GEOS-2, 1971-ISAGEX, 1972-EPSOC/SAFE, 1975-GEOS-3) was planned around Scalar Translocation, some data were taken in each of these programs that could be analyzed by use of this technique. Therefore, the first step was to investigate available laser data archives to obtain a list of events that could be treated. The natural second step was to process some data from these historical archives to obtain a determination of some unique baselines, which will probably not be measured again with satellite techniques. Finally, Lageos was chosen as a useful satellite for Scalar Translocation application.

Lageos was designed to facilitate computation of an accurate orbit. The satellite design and orbit configuration were chosen to minimize the errors in modeling the orbit perturbations. Lageos has a very small area-to-mass ratio, which reduces in size the total perturbation due to non-gravitational forces. The error in representing these forces, either due to lack of knowledge of physical properties of the satellite, the total radiation (direct solar plus albedo), and the atmospheric density, or due to limitations in modeling these forces will be similarly reduced. Lageos also has a high altitude, which reduces the size of orbit perturbations owing to errors and omissions in the gravity field model employed. The high altitude also permits simultaneous or overlapping observations from stations separated by continental distances.

From this variety of data we can then compare and contrast satellites and results, draw some conclusions about analysis of laser tracking data in the Scalar Translocation mode as well as other methods of analysis, and make some recommendations about the usefulness of this approach in the context of the original objective: "development of an operational system to measure and monitor crustal displacement and deformation to support a primary EODAP objective — e.g., the definition of Earthquake Hazard Assessment Models."

3. HISTORICAL DATA

The first laser observations were taken in 1964. Laser tracking systems operated routinely in an organized program for the first time in 1967. At that time, the main objective in making these observations was to obtain a global geocentric datum. However, at that time the relatively poor distribution of laser stations was viewed as a problem, as these stations were located in continental Europe. In fact, for the purposes of Scalar Translocation, this station distribution is quite good. During 1968, two stations again operated in Europe, which was quite good for Scalar Translocation. During 1969 and 1970 there was no major tracking effort. This was a period where programs were being consolidated, and tracking stations were improved, procured, and deployed in support of the final phase of the National Geodetic Satellite Program (NGSP). During 1971, a tracking campaign was initiated that had a more global coverage of laser stations, with the consequence that fewer opportunities existed to obtain "Scalar Translocation" data. With the exception of brief periods during SAFE, 1972 and 1974, little "Scalar Translocation" data were obtained. In 1975, data taken in the calibration area for the GEOS-3 satellite provided many suitable events. The 1976 SAFE data added to the data base. Also, the launch of Lageos in 1976 provided data over longer baselines because of its significantly greater altitude. Therefore, some laser stations, previously treated as separate sites, began to make simultaneous observations.

During the decade from 1967 to 1977, substantial improvements were made in laser technology and in our understanding of the error sources in laser data. The early data achieved 2- to 5-m accuracy with 1 millisecond epoch timing whereas recent data provide a range accuracy of 10 cm and an epoch accuracy of 1 μsec.

During this decade more care has been taken in the design of retroreflector arrays mounted on satellites. By careful analysis, the effective reflecting point from the satellite center of mass can be calculated.

With successive satellites, this correction can be made with increasing accuracy; the early satellite 6508901 had an accuracy of 0.10 m and the latest, 7603901 (Lageos), an accuracy of 0.003 m (Arnold, 1972, 1974, 1975a,b 1978). The satellites with laser tracking data are listed in Table 1. The magnetically stabilized satellites can only be observed in the northern hemisphere. The relative signal strength is given.

Signal strength is directly related to accuracy. With multiple photo-electron events improved accuracy is obtained by using pulse processing of some kind to refer the light travel time to the centroid of the pulse rather than to the leading edge (Pearlman et al., 1975).

Many first- and second-generation laser systems (see Weiffenbach and Hamal, 1975) use visual acquisition to point the laser. Therefore a visual magnitude brighter than 10th magnitude is necessary. Faint satellites such as Starlette and Lageos cannot be observed by some systems, even today. The node rate prescribes how rapidly the satellite geometry changes. Satellite orbit geometry of course affects visibility for visual acquisition. More important however is the orientation of the satellite pass to the station-to-station baseline. As we shall see, the optimum geometry is obtained when the baseline is parallel to and lies in the orbital plane. Therefore, for planning an observing program, the change in orbit geometry must be a factor. The area-to-mass ratio controls the amount of nongravitational acceleration experienced by the satellite, which is important for making predictions for the observation program and reducing the orbit error during data reduction.

The Scalar Translocation events available are indicated in Table 2. The station numbers are identified in Table 3, where the nominal geocentric coordinates are given. These geocentric coordinates are a homogenized set, and are obtained in the following way.

Table 1. Geodetic satellites equipped with laser cube corner reflectors.

Satellite Identification		Stabilization	a (mm)	e	I°	q km	C.M. Reduction Accuracy	Relative Signal Strength	Visual Magnitude	Perigee Rate $\dot{w}$ (°/day)	$\dot{\Omega}$ (°/day)	A/M cm^2/gram
6406401	BE-B	Magnetic	7.360	0.012	80	912	5.	$2\text{-}4\times10^4$	7-9	-2.537	-1.081	0.10
6503201	BE-C	Magnetic	7.503	0.026	41	941	5.	$1\text{-}3\times10^4$	7-11	5.176	-4.256	0.10
6508901	GEOS-1	Gravity	8.074	0.073	59	1121	10.	$0.2\text{-}2\times10^4$	7-10	0.655	-2.247	0.10
6701101	D1-C	Gravity	7.319	0.052	40	579	10.	$0.4\text{-}10\times10^4$	9-10	5.989	-4.744	0.30
6701401	D1-D	Gravity	7.603	0.053	39	569	10.	$0.1\text{-}10\times10^4$	10-11	5.415	-4.244	0.30
6800201	GEOS-2	Gravity	7.708	0.031	105	1101	10.	$0.2\text{-}2\times10^4$	7-10	-1.619	1.402	0.06
7010901	PEOLE	Gravity	6.983	0.017	15	635	10.	$3\text{-}9\times10^4$	5-6	13.345	-7.033	0.20
7501001	Starlette	Sphere	7.335	0.021	50	805	0.5	$3\text{-}7\times10^3$	11	3.306	-3.946	0.0096
7502701	GEOS-3	Gravity	7.222	0.0005	115	840	2.0	10^5	7-8	-.347	2.727	0.04
7603901	LAGEOS	Sphere	12.270	0.0044	109	5888	0.3	20	12-13	-.213	0.343	0.006897

Table 2. Scalar Translocation events.

Year	Stations	6406401	6503201	6508901	6701101	6701401	6800201	7010901	7501001	7502701	7603901	-------
1967	7815, 7816, 7818	X	X	X	X	X						
1968	7815, 7804	X	X	X	X	X	X					
1969	———											
1970	———											
1971	7809, 7804			X			X					
1972	7061, 7080		X	X			X					
1973												
1974	7061, 7080, 7921		X	X			X					
1975												
1976	7061, 7063, 7067, 7068, 7069,		X	X			X		X	X	X	
1977	7080, 7082, 7907, 7921		X	X			X		X	X	X	

Table 3. SAO station coordinates used (geocentric.)

STA	X(MM)	Y(MM)	Z(MM)	LOCATION	
7061	-2.4288306	-4.7997531	3.4172747	SAN DIEGO, CALIFORNIA	NASA
7063	1.1307118	-4.8313719	3.9940900	GODDARD SPACF FLIGHT CFNTER, MARYLAND	NASA
7067				BERMUDA ISLAND	NASA
7066				GRAND TURK ISLAND	NASA
7069				PATRICK AFB, FLORIDA	NASA
7080	-2.5168977	-4.1988464	4.0764145	QUINCY, CALIFORNIA	NASA
7082	-1.7360010	-4.4250506	4.2414331	BEAR LAKE, UTAH	NASA
7804				SAN FERNANDO, SPAIN	CNES
7815	4.5783681	.4579858	4.4031510	HT. PROVINCE, FRANCE	CNES
7816	4.6543431	1.9592004	3.8843797	STEPHANIE, GRFECF	CNES
7907	1.9427877	-5.8040801	-1.7969196	AREQUIPA, BRAZIL	SAO
7921	-1.9367636	-5.0777058	3.3319226	MT. HOPKINS, ARIZONA	SAO
7929	5.1864655	-3.6538602	-.6543223	NATAL, BRAZIL	SAO

A recent set of coordinates for seven stations derived at Goddard Space Flight Center (GSFC) based on Lageos tracking data was adopted. The set of coordinates given by Learch et al. (1977) for 146 stations was then related to this fundamental set by using the five stations common to both sets and computing the transformation parameters, in the sense,

$$T\ (\Delta x,\ \Delta y,\ \Delta z,\ \varepsilon_x,\ \varepsilon_y,\ \varepsilon_z,\ S)\ \overline{X}_{GEM10} = \overline{X}_{Lageos} \quad ,$$

where T is the linear transformation matrix. The remaining coordinates are taken from Gaposchkin (1974). These were related to the fundamental LAGEOS system by taking the 23 stations common to the GSFC homogenized system, computing transformation parameters in the sense,

$$T\ (\Delta x,\ \Delta y,\ \Delta z,\ \varepsilon_x,\ \varepsilon_y,\ \varepsilon_z,\ S)\ \overline{X}_{SAO} = \overline{X}_{Lageos} \quad .$$

Coordinates for a station are given in Table 3 if that station has a simultaneous event with another station used in this analysis. Not all combinations of these stations have suitable simultaneous events. Table 4 gives the transformation parameters.

Table 4. Transformation parameters.

	Δx (m)	Δy (m)	Δz (m)	ε_x (arc sec)	ε_y (arc sec)	ε_z (arc sec)	S (ppm)
Coordinate Systems							
GEM10-Lageos	-1.80	-2.16	-2.00	0.1799	-0.0024	10.2475	0.016
SAO-GEM10	- .08	- .36	+9.69	-0.0328	-0.0823	0.7200	0.257
SAO-Lageos	-1.88	-2.52	7.69	0.1471	-0.0897	0.9675	0.2730

Finally, in Table 5, the number of individual events for each pair of station baselines, for each satellite, for each year is given. For 1976, statistics for 7603901 (Lageos) only have been assembled. However, some passes may not be useful because of bad data or poor pass geometry.

Table 5. Possible overlapping events.

Station Pair		Year	Satellite 6406401	6503201	6508901	6701101	6701401	6800201	7010901	7501001	7502701	7603901
7815	7816	1967	13	26	45	37	56					
7816	7818		1	-	-	5	22					
7815	7818		6	3	3	9	28					
7804	7815	1968	6		13	7	19	22				
7804	7809	1971	2	2	7	11	2	3				
7061	7921	1972		3								
7061	7080	1972		46	8			4				
7907	7929				2							
7907	7929	1973		2	9							
7907	7929	1974		2	12							
7061	7080	1974		24	2			1				
7061	7063	1974		10								
7061	7921	1974		20				6				
7063	7090	1974		2								
7063	7921	1974		2								
7080	7921	1974		3				1				
7063	7067	1975		8	3					1	18	
7063	7068	"		2	8			4		2	31	
7067	7068	"		11	9			9		6	42	
7063	7921	"		5	2						1	
7068	7907	"			3						2	
7819	7842	"			1							
7819	7804	"									6	
7907	7929	"		2	7							
7061	7080	1976										7
7061	7082	"										12
7061	7907	"										5
7061	7921	"										18
7080	7082	"										3
7080	7921	"										2
7082	7907	"										3
7082	7921	"										8
7907	7921	"										32
7907	7929	"										25

4. ANALYSIS OF DATA

Since no set of observations has been taken specifically for translocation, subsets of the available data (Table 5) were selected to establish some properties of the method. First, we set out to study how well baselines can be determined with data that are poor in quality but have good pass geometry. Second, we will look at the effect of orbit height on the results and compare results derived from a low satellite (6503201) with those from a high satellite (7603901).

A very rich period of data with an accuracy of 1 to 2 m was obtained during the Diadem experiment in 1967. The available satellites were low in altitude but the baseline distances were small, and within several months, a considerable number of overlapping events suitable for Scalar Translocation analysis were obtained (Table 5). We claim that baseline determination using Scalar Translocation is independent of observation range noise and bias provided the data have suitable distribution. From the data in 1967, we can test this claim. Of course the baseline determination will depend critically on the epoch timing. During 1967, epoch timing was known only with an accuracy of 1 msec. To minimize this uncertainty on the result, a data set from two satellites within a limited time interval of 60 days was selected. We assume that over such a short time clock drift was small and that whatever the constant error is, it will be the same for all the results. Since we are going to compare only the internal consistency of solutions, such errors will not be a factor.

From the available data, two satellites provided data with reasonable geometry in that time interval (6503201, 6508901). Two orbital arcs were computed for each satellite. The volume of data from the two stations (7815, 7816) including nonoverlapping passes was sufficiently large to determine a satisfactory orbit from those data alone.

The results from 33 events are listed in Table 6. To understand the results we give plots of range residuals after the fitting. Figure 1a gives the residuals for an event with good solution. In Figure 1b detailed computer printout for this event is shown. An event is considered good when the condition number of the variance-covariance matrix is small, the formal standard error is small, the arcs overlap, and the data from each station are symmetrical about the point of closest approach (PCA). From Appendix A, we hold that a small condition number results with strong geometry, i.e., the satellite path is parallel to the baseline. Further, the idea of translocation provides that the orbit error, common to both arcs, cancels out. Then, the larger the part of both arcs that is common to each, the smaller the effect of orbit error. Finally, the most efficient averaging of system bias, orbit scale error, and noise occurs when each pass is symmetrical about the PCA. The plots, such as Figure 1a, obtained from each pass are used as a diagnostic tool to choose passes that are favorable for Scalar Translocation. The time base on these plots is the same for both stations; poor pass geometry and noisy data can be quickly identified.

The baseline distance determined from each satellite is given in Table 7 with the combined result.

Table 7. Translocation results for 7815-7816 baseline.

Satellite	7815-7816 Baseline (m)	σ (m)	n
6503201	1590135.908	±0.599	10
6508901	1590138.399	± .608	22
combined	1590137.050	±0.479	32
EU 50 datum	1590129.96	±3.18	
EU 50 scaled	1590132.81	±3.31	

SOLUTION SUMMARY FOR STATION PAIR 7815 7816

FIX ELEMENTS 3 6 0 0 0 0

COVARIANCE MATRIX IN SPECIAL COORDINATE SYSTEM

2.75887E-01	-2.70049E-03	-5.67552E-02	-8.95704E-02	-5.91505E-01
-2.70049E-03	9.99657E-01	3.82672E-01	6.03928E-01	3.98823E+00
-5.67552E-02	3.82672E-01	1.13988E+00	7.77154E-02	1.80219E+00
-8.95704E-02	6.03928E-01	7.77154E-02	5.40976E-01	2.84419E+00
-5.91505E-01	3.98823E+00	1.80219E+00	2.84419E+00	1.87825E+01

ERROR CODE IS 0

EIGENVALUES

6.49417E-02	7.01033E-02	3.35959E-01	1.00563E+00	2.02623E+01

CONDITION NUMBER 3.120E+02

EIGENVECTORS

2.44451E-01	4.79575E-01	-8.42250E-01	-7.34011E-05	-2.94382E-02
-3.78637E-01	-7.28719E-01	-5.32018E-01	1.49438E-02	2.05755E-01
-1.83738E-01	1.01568E-01	1.25189E-03	-9.73037E-01	9.55105E-02
-8.41647E-01	4.69773E-01	1.81022E-02	2.22281E-01	1.45627E-01
2.33985E-01	8.92883E-02	8.51039E-02	5.97260E-02	9.62533E-01

FORMAL SIGMA OF BASELINE = 1.237 METERS

SQUARE ROOTS OF DIAGONAL ELEMENTS

5.252E-01
9.998E-01
1.068E+00
7.355E-01
4.334E+00

CORRELATION MATRIX IN SPECIAL COORDINATE SYSTEM

1.0000E+00	-5.1422E-03	-1.0121E-01	-2.3185E-01	-2.5985E-01
-5.1422E-03	1.0000E+00	3.5848E-01	8.2124E-01	9.2040E-01
-1.0121E-01	3.5848E-01	1.0000E+00	9.8966E-02	3.8949E-01
-2.3185E-01	8.2124E-01	9.8966E-02	1.0000E+00	8.9226E-01
-2.5985E-01	9.2040E-01	3.8949E-01	8.9226E-01	1.0000E+00

SOLUTION VECTOR IN GEOCENTRIC SYSTEM

1.1610E-06 -2.1407E-06 1.8469E-06 -1.0051E-06 -1.1145E-05 3.7660E-06 6.6446E-06

INITIAL BASELINE	1.590145146
PRELIMINARY NEW	1.590135915
SCALE IN METERS	.000001057
FINAL BASELINE	1.590136972
FINAL-INITIAL	-.000008174

Figure 1a.

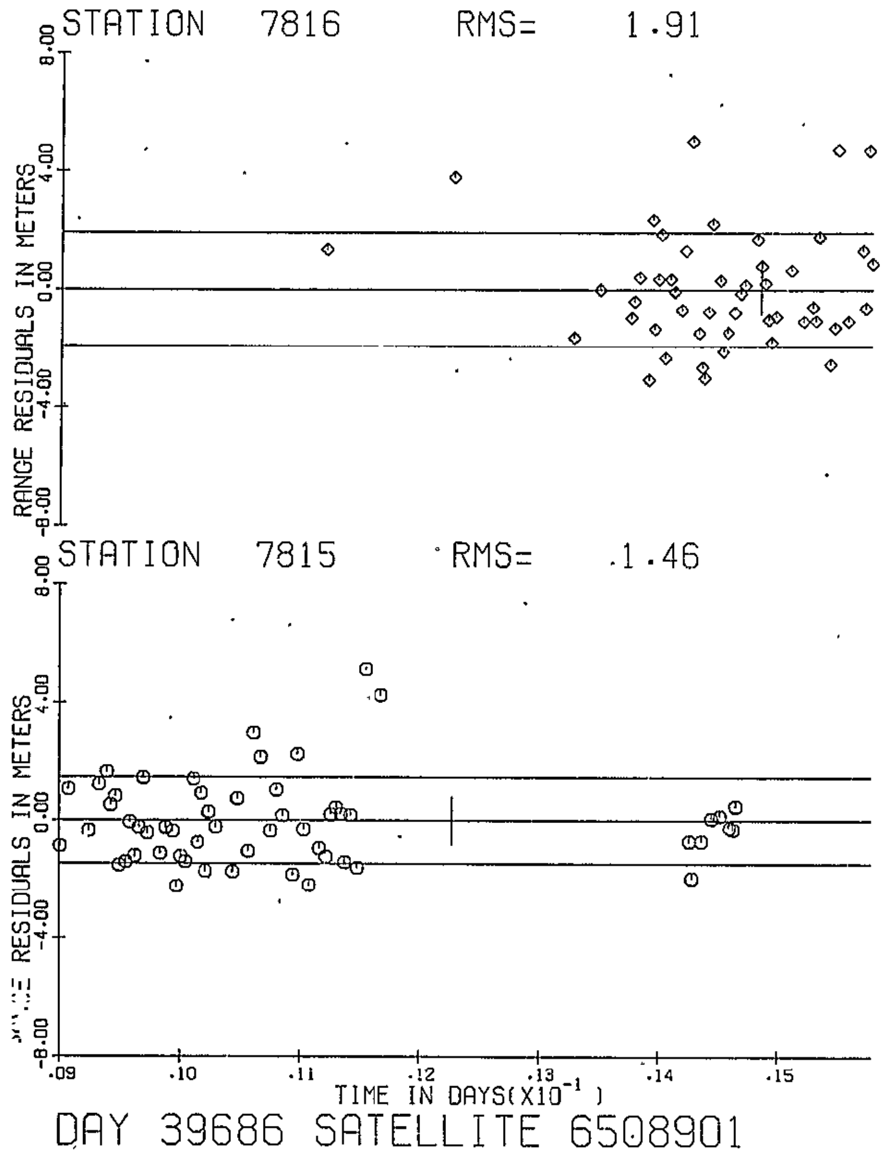

Figure 1b. Plot of range residuals versus time for Geos A after adjustment by the translocation method. The baseline is between 7815 and 7816 (units: meters and days).

Table 6. SAO Scalar Translocation Program.

THERE WERE 33 EVENTS

SOLUTION WEIGHTED IS 1590137.050 +- .479 METERS WITH 32 OBSERVATIONS, SIGMA ZERO IS 2.665

SOLUTION UNWEIGHTED IS 1590137.994 +- .741 METERS WITH 33 OBSERVATIONS, RMS IS 4.192 METERS

7815	7816	6503201	39654.088410	1.388	14	1.279	92	1590140.949	4.156	3.899	2.955	
7815	7816	6503201	39654.977890	1.416	170	1.843	112	1590134.495	.365	-2.555	-3.499	
7815	7816	6503201	39655.057250	1.391	115	1.712	101	1590135.846	.415	-1.204	-2.148	NO OVERLAP
7815	7816	6503201	39655.871980	1.467	101	1.515	88	1590133.651	.743	-3.399	-4.343	
7815	7816	6503201	39655.951130	1.758	110	1.432	99	1590135.317	.516	-1.733	-2.677	
7815	7816	6503201	39657.001130	1.308	147	1.516	132	1590137.441	.288	.391	-.553	
7815	7816	6503201	39657.079930	1.606	48	1.504	93	1590137.529	.661	.479	-.465	
7815	7816	6503201	39659.917790	1.493	95	1.293	111	1590134.917	.574	-2.133	-3.077	
7815	7816	6503201	39648.020440	1.298	23	1.266	71	1590136.798	1.247	-.252	-1.196	
7815	7816	6503201	39651.013590	1.331	68	1.659	121	1590130.331	.684	-6.719X	-7.663	
7815	7816	6503201	39652.062840	1.341	172	1.207	129	1590135.966	.257	-1.084	-2.028	
7815	7816	6508901	39650.984993	1.412	103	2.037	169	1590146.852	2.117	9.802	8.858	
7815	7816	6508901	39651.988131	1.396	78	1.588	143	1590147.324	1.769	10.274	9.330	
7815	7816	6508901	39653.992650	1.762	178	1.589	27	1590149.131	2.318	12.081	11.137	
7815	7816	6508901	39654.995805	1.676	173	1.669	12	1590133.268	3.587	-3.782	-4.726	
7815	7816	6508901	39656.913946	1.709	70	1.953	242	1590138.780	3.531	1.730	.786	
7815	7816	6508901	39659.925723	1.418	144	1.707	49	1590132.390	1.561	-4.660	-5.604	
7815	7816	6508901	39661.932321	1.149	202	1.387	13	1590131.750	1.492	-5.300	-6.244	
7815	7816	6508901	39662.846453	1.572	14	2.130	146	1590142.898	12.536	5.848	4.904	
7815	7816	6508901	39664.853716	1.537	132	1.778	92	1590135.753	2.337	-1.207	-2.241	
7815	7816	6508901	39679.074689	1.249	134	1.118	42	1590139.753	1.107	2.703	1.759	
7815	7816	6508901	39679.991060	1.341	59	1.300	34	1590137.133	.987	.083	-.861	
7815	7816	6508901	39680.993850	1.422	57	1.483	86	1590138.609	.794	1.559	.615	
7815	7816	6508901	39681.998045	1.351	36	1.357	126	1590136.752	.691	-.298	-1.242	
7815	7816	6508901	39684.003504	1.246	44	1.631	10	1590139.715	1.028	2.665	1.721	NO OVERLAP
7815	7816	6508901	39685.007384	1.272	34	1.279	109	1590138.052	.617	1.002	.058	
7815	7816	6508901	39685.923389	1.161	24	2.210	36	1590141.673	3.249	4.623	3.679	NO OVERLAP
7815	7816	6508901	39686.009627	1.469	56	1.914	48	1590136.972	1.237	-.078	-1.022	
7815	7816	6508901	39687.011787	1.170	108	1.894	24	1590136.602	1.569	-.448	-1.392	
7815	7816	6508901	39687.929561	1.037	25	2.164	68	1590140.610	1.505	3.560	2.616	
7815	7816	6508901	39688.932317	.998	28	1.233	98	1590139.105	1.176	2.055	1.111	
7815	7816	6508901	39689.936948	1.048	18	2.371	99	1590140.673	2.166	3.623	2.679	
7815	7816	6508901	39696.869593	1.200	56	1.282	169	1590136.766	.450	-.284	-1.228	

This result can also be compared with the datum coordinates of these stations. The Europe 50 coordinates for these two stations are taken from Gaposchkin (1973). The Europe 50 datum is assumed to have an uncertainty of 2 m. To compare the datum coordinates to a global set, the datum coordinates must be scaled. The scale difference (Gaposchkin, 1974) is 2.6 ± 0.92 m, with the datum scale smaller than that of the satellite. However, the latter was derived from satellite data using a method of analysis that obtained scale from the value of the velocity of light c and the value of GM. The values used in Gaposchkin (1974) were

$$GM = 3.986013 \times 10^{20} \ cm^3/sec^2$$

$$c = 2.997925 \times 10^{10} \ cm/sec \quad .$$

The best present values for these constants are

$$GM = 3.986005 \times 10^{20} \ cm^3/sec^2$$

$$c = 2.99792458 \times 10^{10} \ cm/sec$$

Thus, we correct the satellite scale by

$$\frac{1}{3} \frac{\delta GM}{GM} + \frac{\delta c}{c} = -0.809 \ ppm$$

and derive a correction to the Europe 50 datum baseline of 1.79 ± 0.92 ppm.

Clearly the Europe 50 datum coordinates are the weakest link in this comparison. Nevertheless, the internal consistancy of the baseline solutions from both satellites and the overall agreement to nearly a 1-sigma level with the datum coordinates are satisfactory. Analysis of all the data would further improve the baseline determination.

At this point we can summarize the results.

1) Scalar Translocation works with low-accuracy data: The effects of bias and noise are minimized by the method.

2) The results of Scalar Translocation used on satellites with different orbital characteristics (inclination and eccentricity) are compatible.

3) With suitable observing schedules, the necessary data for submeter baseline determination can be obtained within 60 days or less.

4) Passes with bad geometry (i.e., with the orbit motion perpendicular to the baseline vector) cannot be fit in the translocation mode with reasonable results. Those cases are generally rejected by the linear regression program that determines the final baseline.

5) Translocation computations are excellent for data screening. The orbit fit and station navigation leave residuals that can easily be examined for gross errors on a point by point basis. For example, during reduction of the data, several passes were observed to have multiple returns — i.e., two different but internally consistent sets of residuals. By chosing that set of residuals that best agreed with the a priori baseline distance, the bad data were easily eliminated.

During 1974, laser data were taken in the western United States as part of the San Andreas Fault Experiment (SAFE). The three stations 7061, 7080, and 7921 all participated. Two stations, 7061 and 7080, had data accuracy approaching 10 cm and station 7921 had an accuracy of about 1 m. The station locations are shown in Figure 2. The data taken in SAFE were not optimized for translocation. Most of the data was obtained on satellite 6503201, which has an inclination of I = 39°. Since this inclination is comparable to the latitude of these stations, the observations were made with the satellite at its maximum latitude and, therefore, as it passed from west to east. Such geometry is very strong for line 7061-7921, which is roughly west to east. However, the north-south baseline (7061-7080) is normal to the satellite motion and we would not expect such a strong geometry and, hence, a

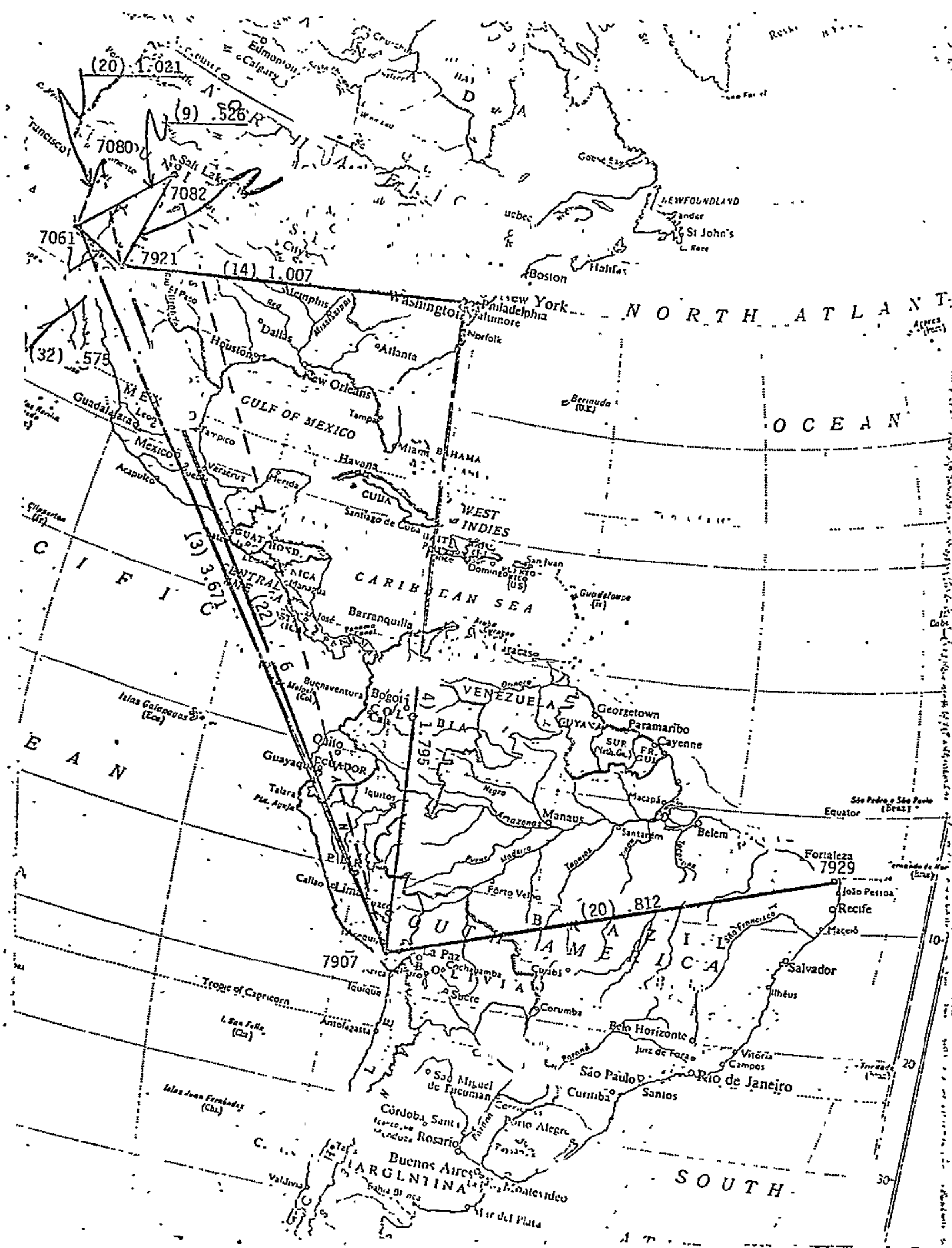

Figure 2. Locations of stations observing during 1976.

weaker solution. Fewer observations on other satellites exist for these lines, but they are also analyzed. So, for the strongly determined baseline (7061-7921), the data from one station (7921) are not so accurate, whereas, where we have accurate data from both stations (7061-7080) the geometry is not strong. Both considerations will be a factor for any method of analysis, not only for Scalar Translocation.

For the 1974 data, 47 events were analyzed. The list of individual baseline determinations and the solutions are given in Tables 8 and 9. Figure 3 is a plot of the post-fit residuals for station pair 7061-7921 and Figure 4 is for station 7061-7080. We summarized the results in Table 10 for the 1974 data.

Table 8. SAO Scalar Translocation Program.

THERE WERE 21 EVENTS

SOLUTION WEIGHTED IS 896273.938 +- 1.050 METERS WITH 17 OBSERVATIONS, SIGMA ZERO IS 4.199

SOLUTION UNWEIGHTED IS 896273.009 +- .791 METERS WITH 21 OBSERVATIONS, RMS IS 3.537 METERS

7061	7080	6503201	42316.717630	.500	140	3.663	56	896267.902	1.734	-6.036	-5.107
7061	7080	6503201	42320.604277	.446	88	2.375	46	896272.176	.971	-1.762	-.833
7061	7080	6503201	42320.683730	.178	125	.721	80	896266.975	.409	-6.963X	-6.034
7061	7080	6503201	42321.655223	.281	60	.265	129	896268.410	.182	-5.528X	-4.599
7061	7080	6503201	42331.575790	.126	53	.457	53	896272.376	.252	-1.562	-.633
7061	7080	6503201	42332.417430	.533	56	.673	61	896268.736	.476	-5.202	-4.273
7061	7080	6503201	42331.367894	.507	102	.191	64	896267.395	1.016	-6.543	-5.614
7061	7080	6503201	42331.526241	.183	129	.306	103	896270.342	.080	-3.596X	-2.667
7061	7080	6503201	42332.337190	.557	136	.685	91	896275.032	.613	1.094	2.023
7061	7080	6503201	42336.383174	.470	113	.558	157	896271.348	.344	-2.590	-1.661
7061	7080	6503201	42336.465600	.239	55	.128	12	896277.726	.942	3.788	4.717
7061	7080	6503201	42337.354750	.297	81	.179	32	896278.087	.167	4.149X	5.078
7061	7080	6508901	42331.248680	.385	48	.101	53	896277.035	.461	3.097	4.026
7061	7080	6508901	42321.395480	.294	28	.103	18	896273.728	1.538	-.210	.719
7061	7080	6508901	42331.248680	.385	48	.101	53	896278.503	.463	4.565	5.494
7061	7080	6800201	42295.472020	.116	69	.157	12	896275.475	.134	1.537	2.466
7061	7080	7603901	43077.462761	.126	203	.164	29	896274.741	.469	.803	1.732
7061	7080	7603901	43085.181262	.115	79	.297	42	896275.395	5.513	1.457	2.386
7061	7080	7603901	43088.256250	.154	566	.168	20	896274.991	.712	1.053	1.982
7061	7080	7603901	43102.091448	.170	458	.197	12	896273.058	1.557	-.860	.049
7061	7080	7603901	43104.124900	.102	135	.159	51	896273.762	.775	-.176	.753

Table 9. SAO Scalar Translocation Program.

THERE WERE 42 EVENTS

SOLUTION WEIGHTED IS 571553.307 +- .327 METERS WITH 42 OBSERVATIONS, SIGMA ZERO IS 2.092

SOLUTION UNWEIGHTED IS 571553.495 +- .442 METERS WITH 42 OBSERVATIONS, RMS IS 2.832 METERS

7061	7921	6503201	42336.305186	.130	52	2.331	26	571554.445	.653	1.138	.950
7061	7921	6503201	42336.465255	.569	137	1.442	27	571552.873	1.898	-.434	-.622
7061	7921	6503201	42337.354750	.230	80	1.019	37	571552.679	.579	-.628	-.816
7061	7921	6503201	42337.433690	.411	121	1.171	39	571548.829	.916	-4.478	-4.666
7061	7921	6503201	42345.205300	.112	7	1.459	22	571554.128	.638	.821	.633
7061	7921	6503201	42345.284910	.265	53	1.396	31	571552.857	.777	-.450	-.638
7061	7921	6503201	42345.365000	.171	32	1.353	30	571551.490	.692	-1.817	-2.005
7061	7921	6503201	42388.499283	.414	133	.766	10	571553.916	3.339	.609	.421
7061	7921	6503201	42388.365255	.144	69	2.155	13	571547.869	1.078	-5.438	-5.626
7061	7921	6503201	42390.442084	.783	80	2.162	18	571548.483	3.720	-4.824	-5.012
7061	7921	6503201	42391.334970	.643	154	2.109	30	571552.460	2.328	-.847	-1.035
7061	7921	6503201	42391.413200	.792	164	1.843	38	571550.078	2.162	-3.229	-3.417
7061	7921	6503201	42391.493230	.155	126	1.267	33	571551.044	.506	-2.263	-2.451
7061	7921	6503201	42391.574600	.175	42	1.233	20	571556.678	.886	3.371	3.183
7061	7921	6503201	42392.385440	.632	149	1.144	41	571548.659	1.642	-4.648	-4.836
7061	7921	6503201	42392.465010	.179	123	1.595	29	571550.564	.725	-2.743	-2.931
7061	7921	6503201	42337.354750	.222	150	1.139	37	571552.123	.590	-1.184	-1.372
7061	7921	6503201	42337.433690	.215	169	1.144	39	571553.189	.509	-.118	-.306
7061	7921	6503201	42388.499280	1.341	56	.968	10	571552.967	10.560	-.340	-.528
7061	7921	6503201	42390.442080	.854	51	2.763	18	571558.446	3.942	5.139	4.951
7061	7921	6503201	42391.334970	.792	51	2.079	30	571560.289	2.589	6.982	6.794
7061	7921	6503201	42391.413200	1.387	55	2.036	38	571557.493	3.293	4.186	3.998
7061	7921	6503201	42391.493230	.632	53	1.286	33	571552.937	1.751	-.370	-.558
7061	7921	6503201	42391.574600	.142	42	.928	20	571553.692	.709	.385	.197
7061	7921	6503201	42392.385430	1.017	49	2.152	41	571559.756	2.276	6.449	6.261
7061	7921	6503201	42392.465010	.613	63	2.119	26	571554.976	2.267	1.669	1.481
7061	7921	6503201	42392.547890	.148	40	1.767	24	571552.393	.703	-.914	-1.102
7061	7921	6503201	42394.406300	1.574	55	2.000	32	571554.632	4.430	1.325	1.137
7061	7921	6503201	42395.299020	1.063	52	1.373	23	571558.548	5.258	5.241	5.053
7061	7921	7603901	43077.462761	.133	204	1.692	106	571555.408	.591	2.101	1.913
7061	7921	7603901	43080.414758	.176	158	.872	73	571553.607	.748	.300	.112
7061	7921	7603901	43081.358421	.151	293	1.198	212	571553.775	.201	.468	.280
7061	7921	7603901	43082.300956	.147	343	.773	123	571553.620	.226	.313	.125
7061	7921	7603901	43082.480730	.120	323	1.042	117	571555.067	.704	1.760	1.572
7061	7921	7603901	43086.366147	.112	343	1.138	111	571555.172	.318	1.865	1.677
7061	7921	7603901	43087.312153	.093	29	1.225	99	571551.490	1.165	-1.817	-2.005
7061	7921	7603901	43089.195313	.107	637	1.573	12	571552.347	1.437	-.960	-1.148
7061	7921	7603901	43090.037414	.119	944	1.482	46	571552.703	.549	-.604	-.792
7061	7921	7603901	43098.449930	.103	26	1.053	53	571556.850	.929	3.543	3.355
7061	7921	7603901	43101.252084	.130	662	1.031	115	571553.499	.274	.192	.004
7061	7921	7603901	43102.226737	.115	101	1.042	65	571551.135	.681	-2.172	-2.360
7061	7921	7603901	43103.309630	.134	878	1.161	85	571553.639	.438	.332	.144

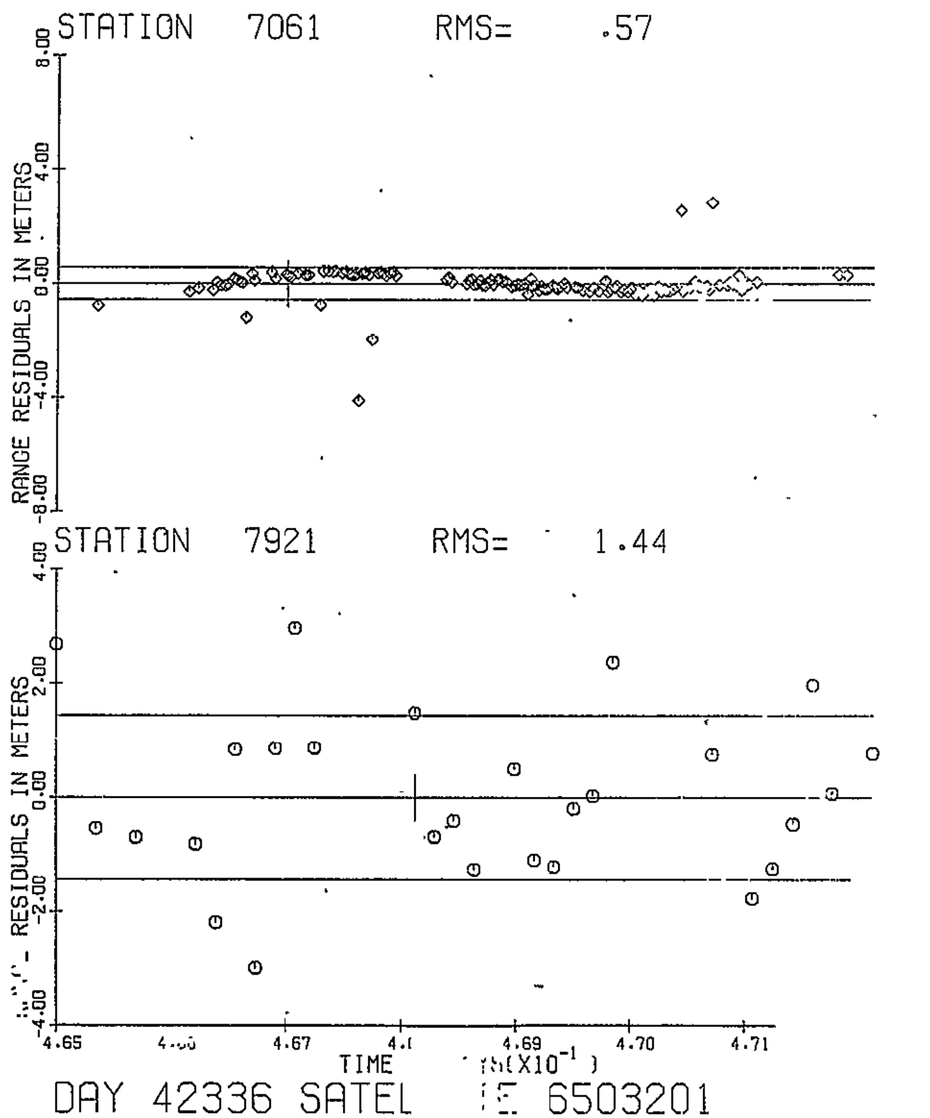

Figure 3. Plot of range residuals versus time for BE-C after adjustment by the translocation method. The baseline is between 7061 and 7921 (units: meters and days).

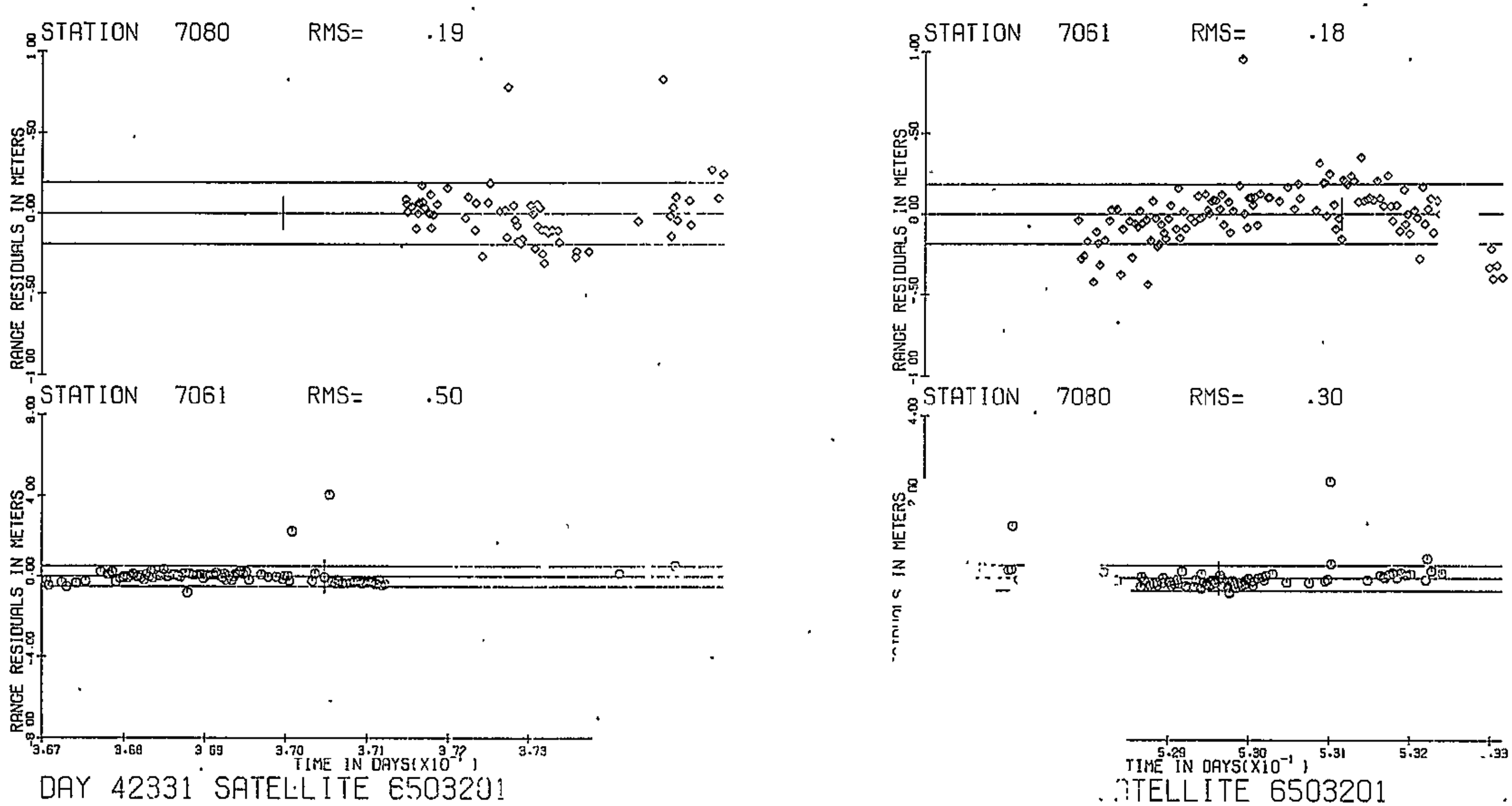

Figure 4a,b. Plot of range residuals versus time for BE-C after adjustment by the translocation method. The baseline is between 7061 and 7080 (units: meters and days).

Table 10. Baseline results for 1974.

Station	Baseline	±		number of events
7061-7080	896272.662	±	1.185	17
7061-7921	571522.354	±	0.460	31

During 1976, the Lageos (7603901) satellite was launched. It is in a significantly higher orbit than any other used in this analysis. LAGEOS was designed to minimize the orbit error due to gravity-field uncertainties, radiation pressure, and drag. It also has an extremely well-defined-center of-mass correction, and it should be an ideal satellite to use for any metric experiment using precision laser ranging data, including Scalar Translocation. The amount of data obtained on Lageos in 1976 is given in Table 5. With such a high satellite, much longer baselines can now be measured, as well as the shorter baselines obtained on lower satellites. The locations of observing stations in 1976 are shown in Figure 2. Of the stations observing, 7061, 7080, and 7082 had an accuracy approaching 10 cm. The stations 7907, 7921, and 7929 had an accuracy of approximately 1 m. Furthermore, 7907, 7921, and 7929 acquired data, almost routinely, from launch and obtained observations for a whole pass — that is, more or less from horizon to horizon. However, stations 7061, 7080, and 7082 obtained data only during a 2-month period in 1976, and many of the passes were partially observed. For example, in Figure 5, three examples are given where only partial passes are observed. Note that on each time line a vertical line is drawn indicating the point of closest approach. In 5 out of 6 passes, the data taken did not cover the midpoint of the pass, which would have strengthened the baseline determination. Due to this data distribution much of the strength of Scalar Translocation has been lost. In Table 11 all baselines determined with 1976 Lageos data are listed.

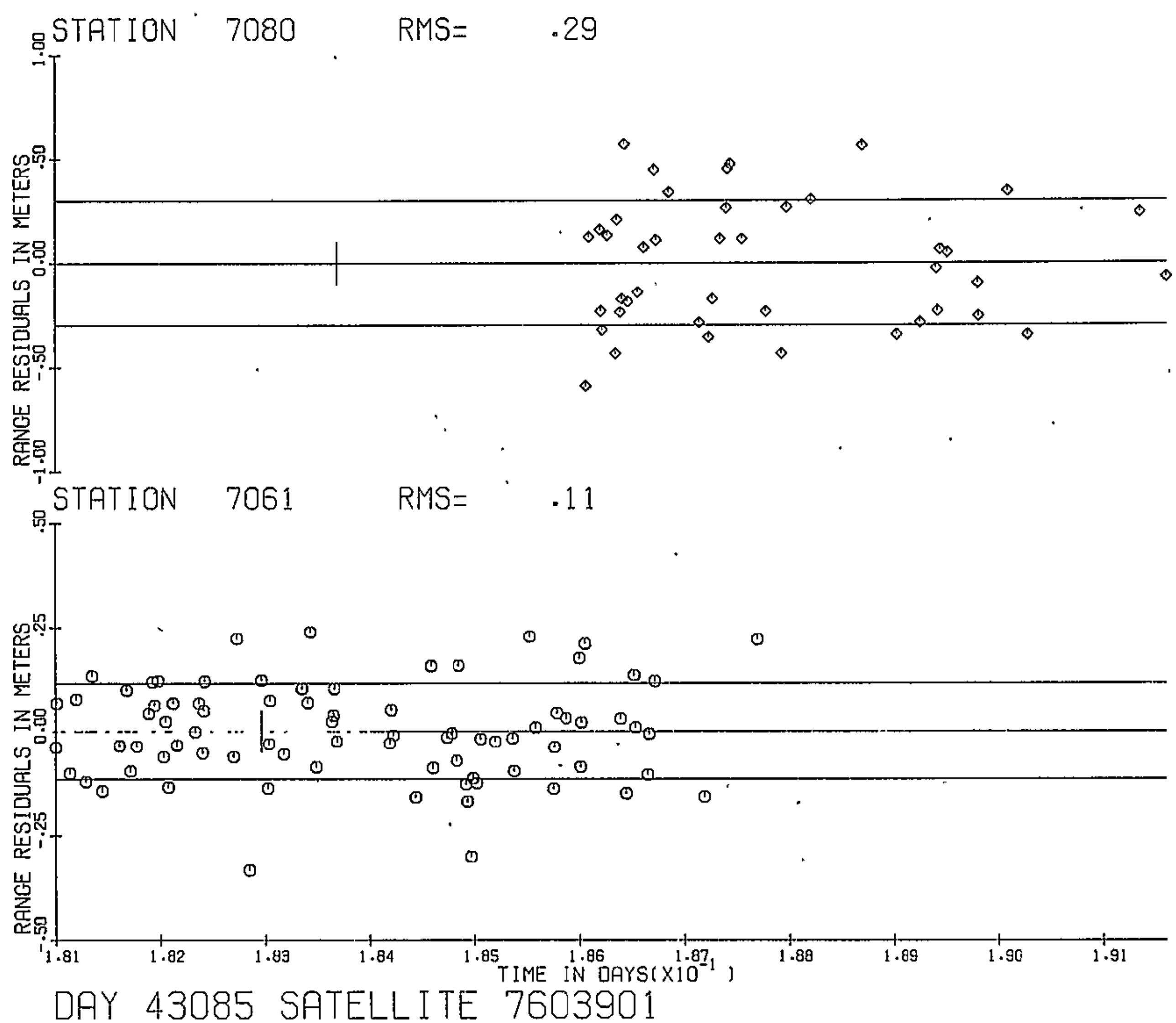

Figure 5a. Plot of range residuals versus time for Lageos after adjustment by the translocation method. The baseline is between 7061 and 7080 (units: meters and days).

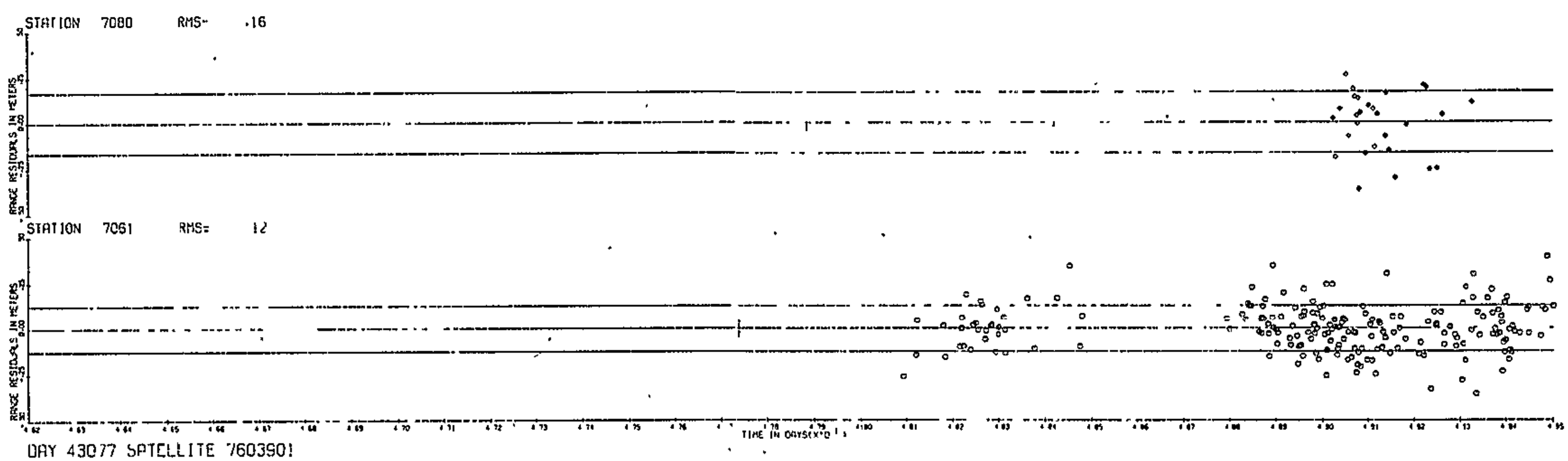

Figure 5b. Plot of range residuals versus time for Lageos after adjustment by the translocation method. The baseline is between 7061 and 7080 (units: meters and days).

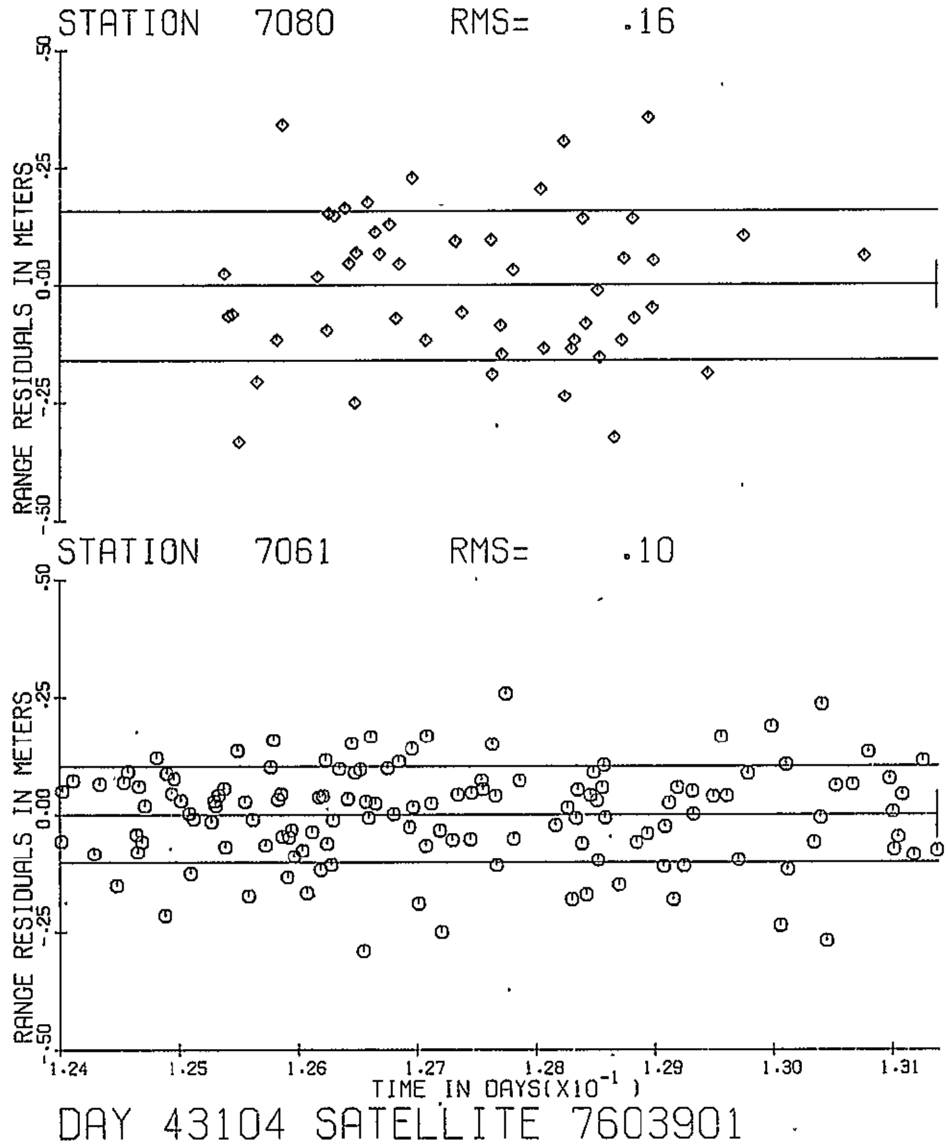

Figure 5c. Plot of range residuals versus time for Lageos after adjustment by the translocation method. The baseline is between 7061 and 7080 (units: meters and days).

Table 11. Baselines from 1976 Lageos data.

Station pair	Baselines		(m)	(n)
7061-7082	1140023.308	±	0.412	7
7063-7921	3147782.230	±	1.631	13
7082-7921	1137309.670	±	0.477	7
7907-7921	6471757.766	±	1.137	16
7907-7929	4055910.642	±	0.513	14

The baselines 7061-7080 and 7061-7921 are determined from the 1974 SAFE data and the 1976 Lageos data. They agree reasonably well. The estimate based on all the determinations is given in Table 12. Table 13 lists each individual baseline determination for the 1977 Lageos data.

Table 12. Combined solution of 1974 and 1976 data.

Station Pair	Baseline	±	m	n
7061-7080	896272.662	±	1.185	19
7061-7921	571553.269	±	0.451	44

As mentioned earlier, and in Appendix A, the power of translocation is hat it reduces the effects of orbit error, observation bias, and noise. To chieve these benefits, good pass geometry and complete distribution about he PCA are necessary. For many of the Lageos passes, the data were incomplete. t is gratifying therefore to obtain such good solutions, even for partial asses. Considerable improvement in baseline determination can be expected hen complete coverage is obtained from all stations with 10-cm data.

Table 13. SAO Scalar Translocation program.

THERE WERE 18 EVENTS

SOLUTION WEIGHTED IS 6471757.766 +- 1.137 METERS WITH 16 OBSERVATIONS, SIGMA ZERO IS 4.402

SOLUTION UNWEIGHTED IS 6471756.793 +- 1.011 METERS WITH 18 OBSERVATIONS, RMS IS 4.167 METERS

7907	7921	7603901	42952.097571	.946	51	1.233	11	6471762.766	8.307	5.000	5.973	NO OVERLAP
7907	7921	7603901	43061.319185	.768	191	1.073	27	6471756.374	.537	-1.392	-.419	NO OVERLAP
7907	7921	7603901	43062.414150	.616	64	.626	59	6471750.973	.524	-6.793	-5.820	
7907	7921	7603901	43063.351563	.646	211	1.081	56	6471754.854	.343	-2.912	-1.939	
7907	7921	7603901	43066.327692	.765	256	1.255	81	6471756.624	.281	-1.142	-.169	
7907	7921	7603901	43067.276042	.899	106	1.259	112	6471759.519	.390	1.753	2.726	NO OVERLAP
7907	7921	7603901	43080.270313	1.162	54	1.116	37	6471748.416	1.578	-9.350	-8.377	NO OVERLAP
7907	7921	7603901	43081.358421	1.419	156	1.191	212	6471752.364	.263	-5.402X	-4.429	
7907	7921	7603901	43082.300956	.989	220	1.044	123	6471758.313	.217	.547	1.520	
7907	7921	7603901	43085.275261	.952	28	1.302	29	6471762.147	1.324	4.381	5.354	NO OVERLAP
7907	7921	7603901	43086.366140	.904	234	1.810	110	6471760.052	.266	2.286	3.259	
7907	7921	7603901	43089.348264	.755	202	1.465	84	6471757.492	.257	-.274	.699	
7907	7921	7603901	43101.252084	.650	136	1.070	115	6471758.292	.233	.526	1.499	NO OVERLAP
7907	7921	7603901	43107.357460	1.521	80	.965	142	6471750.289	.396	-7.477X	-6.504	
7907	7921	7603901	43109.235850	.859	168	1.055	92	6471760.546	.261	2.780	3.753	
7907	7921	7603901	43111.268230	.805	249	1.347	67	6471760.834	.270	3.068	4.041	NO OVERLAP
7907	7921	7603901	43112.220226	.907	82	.922	69	6471759.681	.497	1.915	2.888	NO OVERLAP
7907	7921	7603901	43112.359202	.910	128	1.234	58	6471752.742	.400	-5.024	-4.051	

Table 13. (Cont.)

THERE WERE 14 EVENTS

SOLUTION WEIGHTED IS 4055910.642 +- .513 METERS WITH 14 OBSERVATIONS, SIGMA ZERO IS 1.849

SOLUTION UNWEIGHTED IS 4055910.940 +- .822 METERS WITH 14 OBSERVATIONS, RMS IS 2.965 METERS

7907	7929	7603901	42919.065710	1.333	58	1.016	91	4055912.101	.761	1.459	1.161	
7907	7929	7603901	42922.049210	1.064	78	1.291	37	4055905.899	1.428	-4.743	-5.041	
7907	7929	7603901	42922.984890	1.691	13	1.331	61	4055910.353	2.829	-.289	-.587	
7907	7929	7603901	42927.050868	1.107	55	1.179	50	4055914.244	1.019	3.602	3.304	
7907	7929	7603901	42932.059897	1.475	15	.817	138	4055911.597	1.262	.955	.657	
7907	7929	7603901	42935.034540	1.724	16	1.646	72	4055909.394	2.306	-1.248	-1.546	
7907	7929	7603901	42943.031850	2.048	21	.907	48	4055911.437	2.075	.795	.497	
7907	7929	7603901	42945.053299	.774	18	1.563	79	4055906.904	2.939	-3.738	-4.036	
7907	7929	7603901	42945.992534	1.476	90	.722	184	4055910.855	.365	.213	-.085	
7907	7929	7603901	42948.980382	1.331	49	.827	16	4055917.186	5.066	6.544	6.246	NO OVERLAP
7907	7929	7603901	42951.008160	.985	123	.860	78	4055909.705	.445	-.937	-1.235	
7907	7929	7603901	42956.963368	1.389	14	.511	30	4055915.238	2.833	4.596	4.298	NO OVERLAP
7907	7929	7603901	42958.993316	1.292	17	1.015	134	4055908.960	.862	-1.682	-1.980	
7907	7929	7603901	43088.256250	.996	121	1.532	88	4055909.289	1.706	-1.353	-1.651	

Table 13. (Cont.)

THERE WERE 3 EVENTS

SOLUTION WEIGHTED IS 8286009.579 +- 1.587 METERS WITH 3 OBSERVATIONS, SIGMA ZERO IS 2.244

SOLUTION UNWEIGHTED IS 8286010.265 +- 3.720 METERS WITH 3 OBSERVATIONS, RMS IS 5.261 METERS

7921	7929	7603901	43083.243317	.790	59	1.360	72	8286009.479	.762	-.100	-.786	NO OVERLAP
7921	7929	7603901	43085.275261	1.325	29	1.609	18	8286017.065	3.218	7.486	6.800	NO OVERLAP
7921	7929	7603901	43089.195313	1.607	12	1.242	52	8286004.250	2.428	-5.329	-6.015	NO OVERLAP

THERE WERE 8 EVENTS

SOLUTION WEIGHTED IS 6878048.101 +- 3.014 METERS WITH 7 OBSERVATIONS, SIGMA ZERO IS 7.384

SOLUTION UNWEIGHTED IS 6878048.477 +- 1.442 METEPS WITH 8 OBSERVATIONS, RMS IS 3.816 METERS

7061	7907	7603901	43073.370313	.076	11	.645	186	6878052.575	.212	4.474	4.098	NO OVERLAP
7061	7907	7603901	43076.347223	.139	222	3.104	225	6878042.283	.290	-5.818	-6.194	NO OVERLAP
7061	7907	7603901	43081.358421	.163	298	1.971	155	6878044.818	.287	-3.283	-3.659	
7061	7907	7603901	43082.300956	.149	344	1.212	220	6878053.264	.158	5.163X	4.787	NO OVERLAP
7061	7907	7603901	43088.256250	.153	566	.937	121	6878049.587	.279	1.486	1.110	NO OVERLAP
7061	7907	7603901	43100.304770	.144	472	1.562	277	6878046.665	.257	-1.436	-1.812	
7061	7907	7603901	43101.252084	.131	663	.869	136	6878052.407	.196	4.306	3.930	NO OVERLAP
7061	7907	7603901	43103.281420	.112	712	1.646	191	6878046.221	.166	-1.860	-2.256	

THERE WERE 3 EVENTS

SOLUTION WEIGHTED IS 8711138.206 +- 3.351 METERS WITH 3 OBSERVATIONS, SIGMA ZERO IS 4.739

SOLUTION UNWEIGHTED IS 8711137.861 +- 1.702 METERS WITH 3 OBSERVATIONS, RMS IS 2.408 METERS

7061	7929	7603901	43084.185417	.140	175	1.437	142	8711134.514	.310	-3.692	-3.347	NO OVERLAP
7061	7929	7603901	43089.195313	.107	637	1.570	52	8711140.075	.186	1.869	2.214	NO OVERLAP
7061	7929	7603901	43090.140886	.138	216	1.301	41	8711138.995	.423	.789	1.134	NO OVERLAP

Table 13. (Cont.)

THERE WERE 4 EVENTS

SOLUTION WEIGHTED IS 5928015.899 +- 2.403 METERS WITH 4 OBSERVATIONS, SIGMA ZERO IS 4.161

SOLUTION UNWEIGHTED IS 5928015.806 +- 1.437 METERS WITH 4 OBSERVATIONS, RMS IS 2.488 METERS

7063	7907	7603901	42920.140450	.091	263	1.041	79	5928013.318	.314	-2.581	-2.488	
7063	7907	7603901	42921.086130	.285	760	.923	133	5928018.188	.528	2.289	2.382	
7063	7907	7603901	42926.096934	.144	656	.957	110	5928018.398	.300	2.499	2.592	
7063	7907	7603901	42957.101818	.064	536	.836	17	5928013.319	.580	-2.580	-2.487	NO OVERLAP

THERE WERE 13 EVENTS

SOLUTION WEIGHTED IS 3147782.230 +- 1.631 METERS WITH 13 OBSERVATIONS, SIGMA ZERO IS 5.650

SOLUTION UNWEIGHTED IS 3147783.819 +- 1.103 METERS WITH 13 OBSERVATIONS, RMS IS 3.822 METERS

7063	7921	6503201	42390.444940	.160	155	1.656	16	3147782.656	.940	.426	-1.163	
7063	7921	7603901	42919.204340	.090	55	.768	164	3147778.202	.242	-4.028	-5.617	
7063	7921	7603901	42919.351910	.066	83	.795	169	3147779.818	.352	-2.412	-4.001	
7063	7921	7603901	42920.140450	.089	262	.644	129	3147785.696	.257	3.466	1.877	
7063	7921	7603901	42920.287700	.281	884	.670	64	3147784.190	1.189	1.960	.371	
7063	7921	7603901	42921.235450	.074	672	.724	116	3147779.554	.203	-2.676	-4.265	
7063	7921	7603901	42922.180370	.068	887	.673	33	3147784.011	.514	1.781	.192	
7063	7921	7603901	42922.326590	.135	12	.973	110	3147785.388	.414	3.158	1.569	NO OVERLAP
7063	7921	7603901	42926.246876	.349	925	1.018	58	3147789.200	1.702	6.970	5.381	
7063	7921	7603901	42935.168630	.340	970	.901	15	3147785.967	4.235	3.737	2.148	
7063	7921	7603901	42936.114900	.174	644	1.979	22	3147791.171	1.741	8.941	7.352	
7063	7921	7603901	42939.243400	.108	258	.601	77	3147785.183	.639	2.953	1.364	
7063	7921	7603901	42957.101818	.064	536	.563	19	3147778.606	.766	-3.624	-5.213	NO OVERLAP

THERE WERE 2 EVENTS

SOLUTION WEIGHTED IS 5285874.843 +- .055 METERS WITH 2 OBSERVATIONS, SIGMA ZERO IS .055

SOLUTION UNWEIGHTED IS 5285874.734 +- .129 METERS WITH 2 OBSERVATIONS, RMS IS .129 METERS

7067	7907	7603901	42954.132885	.096	47	.766	16	5285874.606	2.877	-.237	-.129	NO OVERLAP
7067	7907	7603901	42955.070767	.116	59	.956	100	5285874.863	.239	.020	.129	

Table 13. (Cont.)

THERE WERE 4 EVENTS

SOLUTION WEIGHTED IS 829575.611 +- .672 METERS WITH 4 OBSERVATIONS, SIGMA ZERO IS 1.164

SOLUTION UNWEIGHTED IS 829575.069 +- 1.780 METERS WITH 4 OBSERVATIONS, RMS IS 3.083 METERS

7080	7082	7603901	43063.104428	.118	28	.096	8	829578.849	1.558	3.238	3.780	NO OVERLAP
7080	7082	7603901	43065.133221	.066	7	.097	165	829575.430	.272	-.181	.361	
7080	7082	7603901	43095.201970	.201	11	.164	153	829575.741	1.839	.130	.672	
7080	7082	7603901	43095.295226	.112	18	.134	249	829570.257	3.608	-5.354	-4.812	

THERE WERE 2 EVENTS

SOLUTION WEIGHTED IS 7547301.057 +- 3.663 METERS WITH 2 OBSERVATIONS, SIGMA ZERO IS 3.683

SOLUTION UNWEIGHTED IS 7547302.271 +- 3.498 METERS WITH 2 OBSERVATIONS, RMS IS 3.498 METERS

7080	7907	7603901	43088.256250	.168	20	.830	121	7547298.773	.518	-2.264	-3.498	NO OVERLAP
7080	7907	7603901	43095.295226	.112	18	.674	269	7547305.769	1.069	4.712	3.498	NO OVERLAP

THERE WERE 2 EVENTS

SOLUTION WEIGHTED IS 1289662.073 +- 2.796 METERS WITH 2 OBSERVATIONS, SIGMA ZERO IS 2.796

SOLUTION UNWEIGHTED IS 1289659.034 +- 4.934 METERS WITH 2 OBSERVATIONS, RMS IS 4.934 METERS

7080	7921	6503201	42336.465250	.116	13	1.516	20	1289654.100	3.123	-7.973	-4.934
7080	7921	7603901	43077.462761	.163	29	1.214	106	1289663.967	.742	1.894	4.934

THERE WERE 5 EVENTS

SOLUTION WEIGHTED IS 7203954.113 +- 1.246 METERS WITH 3 OBSERVATIONS, SIGMA ZERO IS 1.762

SOLUTION UNWEIGHTED IS 7203956.073 +- 1.388 METERS WITH 5 OBSERVATIONS, RMS IS 2.775 METERS

7082	7907	7603901	43071.336893	.154	288	.838	255	7203961.006	.117	6.893X	4.933	NO OVERLAP
7082	7907	7603901	43093.263369	.166	433	2.153	180	7203953.061	.245	-1.052	-3.012	NO OVERLAP
7082	7907	7603901	43095.295220	.248	248	2.101	273	7203954.258	.365	.145	-1.815	
7082	7907	7603901	43096.244440	.149	584	1.273	176	7203955.072	.246	.959	-1.001	NO OVERLAP
7082	7907	7603901	43100.304770	.132	85	.657	277	7203956.968	.209	2.855X	.895	NO OVERLAP

All regression solutions for baseline were made using the formal uncertainty computed for each event. The standard error of unit weight ranges from 3 to 10, which indicates that in all cases some unmodeled error sources still exist. However, these standard errors are not unreasonably large. Also computed is the baseline, assuming all observations are of the same accuracy. This unweighted average is also given with the residuals derived from this solution. In general, the solutions are in good agreement. The very large residuals in the unweighted solution have a large variance when used in the weighted solution, which reduced their effect on the mean. It can also be noted that the large formal uncertainties correspond to poor pass geometry, sparce data, or noisy data (as reflected in the R.M.S. for the station). The weighted mean is taken as the best estimate of the baseline.

For an assessment of these results, we can make two comparisons given in Table 14. Here we give the baselines as determined from datum coordinates (suitably scaled), the results provided by GSFC (D. Smith, private communication), and the combined results of the Scalar Translocation. The scaling of the datum coordinates for the NAD27 was taken from Gaposchkin (1974). This scale factor of 1.78 ppm is modified by -0.809 ppm to reflect a change to the current best estimates of GM and c. The coordinates derived by GSFC are obtained from analysis of Lageos data in a global, geocentric, dynamical determination of station coordinates. It is based on 31, 5-day arcs of data and much of the Lageos data used here is common to both analyses. Therefore, what good agreement is found for those coordinates or baselines that are determined only from LAGEOS data may be due to use of the same data rather than both solutions being "correct" to that accuracy.

The datum comparisons are useful only as an overall check. For long baselines, satellite determinations are more accurate when they are reliable. In this case we can conclude that the satellite measurements are valid, and that the geodetic coordinates agree with both satellite determinations as well as might be expected.

Table 14. Comparison of baseline determinations.

Station Pair	NAD 27 Baseline (Mm)	Scaled Datum Baseline (m)	GSFC Lageos Coordinates (m)	Translocation Result (m)	n
7061-7080	0.89626931	896270.18	896275.60 ± 0.14	896272.66 ± 1.185	19
7061-7082	1.14001784	1140018.95	1140022.78 ± 0.04	1140023.31 ± 0.41	7
7061-7921	0.57154694	571547.50	571552.89 ± 0.03	571553.27 ± 0.45	44
7082-7921	1.13730284	1137303.94	1137309.89 ± 0.04	1137309.67 ± 0.48	7
7063-7921	3.14778452	3147787.57	3147785.16 ± 0.04	3147782.23 ± 1.631	13
7907-7921			6471750.94 ± 0.03	6741757.77 ± 1.14	16
7907-7929			4055910.23 ± 0.04	4055910.64 ± 0.93	14

Comparison of the dynamical determination (GSFC) with the translocation result immediately shows two facts. The formal statistics differ by an order of magnitude, which is due to the different meaning attached to them. In the case of the dynamical determination, the formal uncertainty is obtained from the root mean square of the orbital residuals. With approximately 100,000 observations, the $1/\sqrt{n}$ is unrealistically reducing the formal uncertainty. Such an overoptimistic formal uncertainty is well known when a large amount of data is used. The Scalar Translocation uncertainty estimate is obtained from comparing the individual baseline estimates. This no longer used the enormous number of data points, though of course all data points were used to get each baseline estimate. In general the two estimates agree within the combined formal uncertainty.

The second point is that the translocation result is systematically larger than the dynamical result. It is not clear from such a small number of baselines if this is a significant difference. If it is, then this difference will have significance in establishing an absolute scale from satellite laser ranging. The translocation method relies totally on the velocity of light to establish a length scale with the light second. Dynamical methods by their nature obtain scale in a complicated mixture of c, GM, and the orbit theory.

5. DISCUSSION

The theory and results presented in this study are intended to establish Scalar Translocation as a viable option for determination of baseline distances with decimeter accuracy. With the data available, this has been established.

Scalar Translocation provides the following features:

1) Is independent of absolute orbit accuracy and GM.

2) Provides scale by laser range measurements.

3) Uses overlapping passes.

4) Is independent of observation bias and noise under certain well understood and simple conditions of data distribution.

To establish further the use of Scalar Translocation for precision metrology, two steps can be considered.

1) Further analysis of existing data is possible. In fact, originally all the data taken in 1975 and 1976 in support of GEOS-3 program was planned for analysis. In that data set, a large number of simultaneous events are recorded in the Western North Atlantic, involving stations at Goddard Space Flight Center, Bermuda, Grand Turk, and Florida. A braced quadrilateral can be computed to provide a needed internal check on the baseline determination.

2) A planned program of observation could be undertaken specifically for Scalar Translocation. The satellites could be chosen to obtain optimum pass geometry, and, if options on station deployment are possible, then optimum network configurations can be chosen. Such a program would be the most effective approach to establishing baselines independent of satellite orbit theory.

Some unresolved issues remain. First is the question of possible systematic differences in scale between translocation and orbital methods. We believe that translocation as applied here, obtains scale directly from laser range data. It is convenient to assume that this difference occurs in the dynamical method because of its inherently greater complexity. However, the sources of this scale difference must be known before we have real confidence that both translocation and dynamical methods are understood.

Next is the issue of the amount of data necessary. Some improvement in baseline determination was obtained by using all the data points available for each pass. One can wonder where the point of diminishing returns sets in. Must we have 500 or 1000 points in a pass to reduce the random error, and cancel the systematic error? Further study is required.

Then we come to the question of how many individual baseline determinations are necessary to obtain a 10-cm accuracy. The largest number of successful baselines where both stations acquired 10-cm data on Lageos with significant overlaps of the data span was seven for stations 7061-7082. In this case, we obtained an uncertainty of 0.41 m. A simple scaling argument indicates that 112 events are necessary to obtain a 10-cm accuracy.

This conclusion then leads to the question of how much time is necessary to obtain such a data set. If we assume a 50% loss of opportunities due to weather, logistics, system failure, etc., and that this loss is uncorrellated at the two stations and that each station has 4 opportunities each day to observe each satellite, then we have one successful event per satellite per day. For short baselines that can obtain overlapping data on low satellites and, say, four satellites are used, then we have

$$\frac{112}{4} \approx 28 \text{ days of data taking.}$$

This could be reduced further if the data loss due to weather was correlated between stations. If the baselines are such that only Lageos can be used then the full 112 days are necessary. In addition, an analysis where the translocation baseline information is combined with the dynamical determination of station locations can be envisioned. The improvement possible using all the data in this way also needs study. Further work on this point is warranted.

6. REFERENCES

ARNOLD, D.A.

1972. Calculation of retroreflector array transfer functions.
Final Technical Report, NASA Grant NGR 09-015-196, December.
[This report gives results computed for satellites BE-B(6406401), BE-C(6503201), Geos 1(6508901), DIC(6701101), DID(6701401), Geos 2(6800201), Peole(7010901), and Geos 3]

1974. Optical transfer function of NTS-1 retroreflector array.
Technical Report RTOP 161-05-02, NASA Grant 09-015-022,
Supplement No. 57,
October.

1975a. Optical transfer function of Starlette retroreflector array.
Technical Report RTOP 161-05-02, NASA Grant NGR 09-015-002,
Supplement No. 57,
February.

1975b. Optical and infrared transfer function of the Geos 3 retroreflector array.
Technical Report RTOP 161-05-02, NASA Grant NGR 09-015-002
Supplement No. 57,
October.

1978. Optical and infrared transfer function of the Lageos retroreflector array.
Technical Report, NASA Grant NGR 09-015-002.
May.

Gaposchkin, E.M.

1974. Earth's gravity field to the eighteenth degree and geocentric coordinates for 104 stations from satellite and terrestrial data.
J. Geophys. Res. Vol. 79, No. 35, pp 5377, 5411.
December 10, 1974.

Latimer, J.H. and Gaposchkin, E.M.
1977. Scalar Translocation using laser range data. Presented at the Spring Annual Meeting of the American Geophysical Union, June. Center for Astrophysics Reprint Series #750.

Lerch, F.J., Klosko, S.M. and Laubscher, R.E.
1977. Gravity model improvement using Geos 3 (GEM 9&10). Presented at the Spring Meeting of the American Geophysical Union, Washington, D. C.
May 31, 1977 55pp.

Pearlman, M.R., Lanham, N.W., Lehr, C.G., and Wohn, J.
1977. The Smithsonian Astrophysical Observatory laser tracking system. Phil. Trans. R. Soc. Lond. A. 284, 431-442.
(1977) 12pp.

Weiffenbach, G.C., and Hamal, K.
1975. Laser tracking instrumentation. Proceedings of 2nd Workshop held at Faculty Nuclear Science and Physical Engineering, Technical University of Prague, Prague, 11-16 August 1975. Publication of the Faculty of Nuclear Science and Physical Engineering, Technical University of Prague, 140pp.

Appendix A.

CENTER FOR ASTROPHYSICS

PREPRINT SERIES

No. 750

SCALAR TRANSLOCATION USING LASER RANGE DATA

James H. Latimer and E. M. Gaposchkin

Presented at the

Spring Annual Meeting of the
American Geophysical Union
Washington, D.C.

June 1, 1977

Center for Astrophysics
60 Garden St.
Cambridge, Massachusetts 02138

Harvard College Observatory   Smithsonian Astrophysical Observatory

Center for Astrophysics
Preprint Series No. 750

SCALAR TRANSLOCATION USING LASER RANGE DATA

James H. Latimer and E. M. Gaposchkin

Smithsonian Astrophysical Observatory, Cambridge, Massachusetts 02138

Presented at the

Spring Annual Meeting of the
American Geophysical Union
Washington, D.C.

June 1, 1977

SCALAR TRANSLOCATION USING LASER RANGE DATA

James H. Latimer and E. M. Gaposchkin

Smithsonian Astrophysical Observatory, Cambridge, Massachusetts 02138

ABSTRACT

Short overlapping arcs of laser data from two stations are used to determine the interstation distance. This distance is relatively uncorrupted by satellite orbital errors and is independent of satellite orbital scale, which is determined by GM. Here, scale is defined by the adopted velocity of light. Several individual such baselines are averaged to give an estimate of the baseline distance. A network of baselines can be adjusted or combined with other types of data to obtain geocentric station coordinates in the FK4 system referred to the Conventional International Origin.

1. INTRODUCTION

The satellite methods used to determine stations positions fall into three categories: geometrical methods, dynamical methods, and semidynamical or short-arc methods. For many years, geometrical methods have been used with simultaneous camera observations* to obtain interstation directions (Veis, 1967; Aardoom, Girnius, and Veis, 1967; Schmid, 1974). Since camera observations are given with respect to a celestial system, absolute directions in space can be determined; but, being directions only, they provide no origin nor scale. These geometrical directions are very powerful when used in combination with other types of data, notably dynamical methods, such as was done with great advantage in constructing the Smithsonian Standard Earth (SE) models SE I, SE II, and SE III (Lundquist and Veis, 1966; Gaposchkin and Lambeck, 1970; Gaposchkin, 1973). Even so, the need that data be simultaneous resulted in a very slow acquisition of successful events because of the restrictions caused by twilight conditions, weather, and other operational considerations.

Camera data have now been supplanted by laser range data, and the analogous geometrical method is called multilateration. To be effective, multilateration requires simultaneous events involving at least six stations, with a minimum of four stations participating in each event; however, owing to weather and logistical factors, successful multilateration events will not occur very frequently. Furthermore, dedication of six laser systems to this one endeavor may not be practical. Multilateration provides no origin, and no orientation of the network, although scale is strongly determined by the adopted value of the velocity of light, c.

---

* In practice, it is virtually impossible to define and obtain a truly simultaneous observation. Since independent time standards can be synchronized only to between 1 and 50 μsec, predicted satellite positions will have uncertainties approaching several meters, or many milliseconds in light travel time. Therefore, we really mean quasi-simultaneous observations with time differences (determined after the fact) small enough that linear interpolation in satellite position is possible. Thus, simultaneous events can be considered as limiting cases of the semidynamical method.

Dynamical methods depend on knowledge of precise ephemerides (Lundquist and Veis, 1966; Gaposchkin and Lambeck, 1970; Gaposchkin, 1973; Anderle, 1974; Smith, Lerch, Marsh, Wagner, Kolenkiewicz, and Kahn, 1976). An ephemeris defines the reference system and can be related to the center of mass of the earth implicitly by adopting a geopotential-force model with $J_1 = 0$. The orientation of the orbit is similarly implicitly defined to be along the axis of maximum moment of inertia by having $\overline{C}_{21} = \overline{S}_{21} = 0$; but in fact, owing to elastic deformation, this is never exactly true. The origin of longitude can be defined for orbit computation only by using observations somehow related to an inertial reference frame, e.g., camera observations referred to a star background.

Therefore, using metric measurements that are invariant under coordinate translation and rotation, we can approximate the center-of-mass coordinates with one undetermined origin of longitude. The scale in dynamical methods is derived from the adopted value of GM, which relates the dynamical scale (the mean motion n) and the geometrical scale (the semimajor axis a) through an appropriate statement of Kepler's third law:

$$n^2 a^3 = GM(1 + \varepsilon) \quad ,$$

where ε, a small parameter, depends on the satellite orbit, the even zonal harmonics, and any nongravitational force affecting the energy of the orbit, such as radiation pressure and atmospheric drag. Since metric measurements imply a scale through the velocity of light, a consistent set of c and GM must be chosen. A value for the velocity of light c has now been adopted by the International Astronomical Union, the International Association of Geodesy, and the International Union of Geodesy and Geophysics (Melchior, 1975):

$$c = 2.99792458 \times 10^{10} \text{ cm/sec}$$

We are thus obliged to determine GM to be consistent with c; the currently accepted best value for GM is

$$GM = 3.986005 \times 10^{20}\ \mathrm{cm}^3/\mathrm{sec}^2 \quad ,$$

where M here includes the mass of the atmosphere.

Semidynamical methods (Brown, 1976; Strange, Hothem, and White, 1975) rely on the use of short arcs and assume that the orbital error can be corrected to fit the data from one station and that the observations from the second station determine that station position with respect to the corrected orbit and therefore with respect to the first station position. This technique has many guises, the most successful being translocation with doppler data. The method described here is a variant of the semidynamical method.

2. OUTLINE OF THE METHOD

We consider a short arc of a satellite trajectory to be less than half a revolution, although trajectories can be computed by using data from a global network of observing stations for a longer interval, say several days. The trajectory will have errors that depend on model errors in the orbit-determination computation due to uncertainties in the geopotential, other geophysical quantities such as tides, atmospheric drag, geocentric station coordinates, and errors in the observations. Trajectory errors — comprising translation, orientation, and scale biases — are more or less constant during a short arc. However, during a short arc, we assume that the shape of the trajectory is known. Therefore, if we consider a trajectory in space, with an arbitrary position and orientation, the observed laser range data from a station can be used to compute the position of the station relative to the trajectory, which is equivalent to correcting the satellite ephemeris. In addition, data from a second station observing the same trajectory can be used in the same way. Both stations are now related to the same arbitrary trajectory, and their relative positions are therefore established. Although the vector difference cannot be interpreted, because the position and orientation of the trajectory are arbitrary and unknown, the scalar distance between the stations is invariant under this unknown translation and rotation and therefore can be interpreted — hence the name scalar translocation.

Each simultaneous, or overlapping, event provides an individual, independent estimate, together with an uncertainty, of the interstation baseline, which can be used in a number of ways. After calculating the standard error of unit weight, a weighted mean of several determinations can give an improved estimate of the baseline and a more reliable estimate of the accuracy. Gross errors can be eliminated by performing a 3 σ or similar test on a number of independent baseline estimates. Alternatively, if the change of a baseline is desired — for example, to study secular (tectonic) or periodic (tidal) motions — then the determinations with their epochs can be analyzed as a time series. In addition, a network of baselines, each obtained with a weighted mean, can be analyzed to obtain the three-dimensional coordinates of the observing sites; the network, of course, would have an arbitrary origin and orientation. For this, the minimum network would have to have four stations, the six baselines forming a braced quadrilateral, with no redundancy. In general, with n stations and all possible interstation distances measured, there will be $(n^2 - 7n + 12)/2$ degrees of freedom in a network adjustment. Finally, the individual baselines can be used in a general network adjustment with other data, such as with interstation directions determined with simultaneous camera observations, very long-baseline-interferometer observations of direction and distance, or normal equations for station coordinates developed by using long-arc orbital analysis. Direction observations can give an orientation to the network with reference to, say, the FK4 or FK5 system of fundamental stars, while orbital analysis can provide an origin related directly to the center of mass of the earth.

2.1 Scale

The two length scales are provided by the speed of light and the value of GM. Distance is obtained with a light-travel-time measurement suitably corrected for refraction. The speed of light has been defined by the International Union of Geodesy and Geophysics in terms of meters and seconds and is known with sufficient accuracy for our needs. Therefore, our unit of length is, in reality, the light second. Satellite motion also has scale through a suitable definition of Kepler's third law, the defining constant being the product of G, the gravitational constant, and M, the mass of the earth. GM is not now known with sufficient accuracy and is almost certainly inconsistent with the adopted value of c. Therefore, the two scales must be separated and reconciled. The determination of GM, given a defined length scale, comprises a study by itself and will not be discussed here.

If, for the moment, we consider satellite motion on a sphere, then an error, or inconsistency, in GM would model the satellite's motion slightly larger or smaller than reality, as shown in Figure 1. Consider observations of distance $\rho_i = \rho(t_i)$. If the shape of the trajectory is known, then barring certain degenerate geometries (Blaha, 1971, 1972), the position of R can be determined. With a scale error in the model, each point on the orbit will increase its geocentric distance by the same amount. For a more general surface, the increase is proportional to the geocentric distance. Also, a change in distance between each pair of points is proportional to the distance. The actual ranges, of course, can then be used to determine the position and the scale factor corresponding to the correction to GM. Alternatively, assuming a scale error in the observation, the constant of proportionality by which all the geocentric distances change could be applied to the observed ranges. This would then scale the position $\overline{R}$ accordingly if the orbital scale is assumed to be correct. In either case, the position $\overline{R}$ and the scale parameter can be determined from the data to make the observed ranges fit the satellite range. These two interpretations of scale are equivalent for each arc, although the observation equations and the numerical solutions, as reflected by the condition number, are significantly different. For purposes of [illegible]cal analysis, we have computed the station position and the scale parameter assuming a scale error in the observed range because the least-squares solution is much better conditioned; the condition numbers are 10^3 to 10^6 smaller. Since the observed ranges are assumed to be without scale error, the scale parameter is identified with an orbital scale error. The consequence is simply that after the adjustment, the scale parameter is then applied to the determined baseline to refer it back to the observed distance scale.

By determining a scale parameter for each arc, the baselines are found to be independent of orbital bias. This bias could be due to an inconsistency between GM and c, to errors in the orbital theory, or to other causes. However, for this analysis, we have decoupled the scale errors from the desired quantity, the baseline distance. Some numerical tests were performed, during which we changed the value of GM in the orbit computation by as much as

±20 ppm. The baselines recovered in this way, from both high (Lageos) and low (BE-C) satellites, were not identical, but they changed by only a few centimeters individually and the mean of several determinations was virtually the same for each.

2.2 Observational Bias

The determination both of satellite positions with respect to an arbitrary trajectory and their relative positions is done by the method of least squares. The data, however, can have biases as well as random errors. If we consider an optimum pass whose subsatellite track is along the direction between the stations (the baseline of interest) and if the data are uniform about the point of closest approach, then bias in the observed range will cancel along the track and the root-mean-square (rms) residuals will increase. Clearly, the satellite-to-station height will also change, but we are not interested in that component here. Numerical tests in which a bias of 1 m was added to the data left the baseline determination unchanged. Of course, for poor geometry, this independence of bias is reduced.

From Figure 2, it is evident that an epoch time offset from one station to the next will translate directly into a baseline change. The error is about 7 mm for each microsecond bias in station timing for close-earth satellites.

2.3 Adjustment Procedures

The adjustment of a station position to the trajectory is, in general, poorly conditioned since the three coordinates are not determined with equal accuracy. To identify the coordinates that are well determined, we created a local terrestrial coordinate system with its origin at one station and its x axis oriented toward the second station. The difference in the correction to the x coordinate is thus the desired correction to the baseline distance.

For the first station, the point of closest approach is identified and the y axis lies in the plane containing the point of closest approach and the x axis; the z axis is the third direction forming the orthogonal rectangular triad. The station is then "navigated" in this system. In general, the z coordinate is very weakly determined (as shown numerically by an eigen-vector/eigen-value analysis) and is deleted from the solution. For the second station, the y axis is also defined by the point of closest approach of the trajectory with respect to the second station, and the z axis is orthogonal to the x and y axes in a similar way. The z coordinate for this station is also generally deleted from the solution. We are left with a least-squares solution for Δx_1, Δy_1, Δx_2, Δy_2, and the scale parameter ε. The correction to the baseline Δr is

$$\Delta r = \Delta x_1 - \Delta x_2 + \varepsilon(x_1 - x_2) \quad .$$

[Note: Δy_1 and Δy_2 are in different coordinate systems. Since these parameters are included only to obtain a satisfactory adjustment, they are not considered further here.]

Because the adjustment depends on the coordinate system, which depends on the positions of the points of closest approach to both stations, the solutions are quite dependent on the geometry: The baseline distance can be determined very well if the satellite's motion is parallel to the interstation direction, but it is poorly determined if the motion is across this line. The limiting worst case is for a straight-line trajectory [illegible]l to the inter-station line; in this degenerate case, there is an infinite number of solutions. In practice, however, the curvature of the satellite trajectory is sufficient to allow a degraded determination even with poor geometry.

2.4 Translocation Mathematics

The observation equation for station 1 is

$$\rho_{i\ (\text{computed})} = \sqrt{(x_1 - x_i)^2 + (y_1 - y_i)^2 + (z_1 - z_i)^2}\,(1 + \varepsilon) \quad , \qquad (1)$$

where i is the observation index; x_i, y_i, and z_i represent the satellite position; x_1, y_1, and z_1 are the station coordinates; ρ_i is the range from the station to the satellite; and ε is the proportional scale change. The same equation holds for station 2 by using x_2, y_2, and z_2 as its coordinates. Equation (1) is the usual metric scaled by the scale factor ε interpreted as an instrumental error (see Section 1).

The linearized form of equation (1) is

$$d\rho_i = \left(\frac{x_1 - x_i}{\rho_i}\right) dx_1 + \left(\frac{y_1 - y_i}{\rho_i}\right) dy_1 + \left(\frac{z_1 - z_i}{\rho_i}\right) dz_1 + \rho_i \varepsilon$$

for observations from station 1, and similarly for station 2. After applying weights, this leads to the following system of normal equations in matrix form, where p_i is the weight of the observation:

$$\begin{bmatrix} \sum_i p_i\left(\frac{x_1 - x_i}{\rho_i}\right)^2, & \sum_i p_i\left(\frac{x_1 - x_i}{\rho_i}\right)\left(\frac{y_1 - y_i}{\rho_i}\right), & \sum_i p_i\left(\frac{x_1 - x_i}{\rho_i}\right)\left(\frac{z_1 - z_i}{\rho_i}\right), & 0, 0, 0, & \sum_i p_i\left(\frac{x_1 - x_i}{\rho_i}\right)\rho_i \\ & \sum_i p_i\left(\frac{y_1 - y_i}{\rho_i}\right)^2, & \sum_i p_i\left(\frac{y_1 - y_i}{\rho_i}\right)\left(\frac{z_1 - z_i}{\rho_i}\right), & 0, 0, 0, & \sum_i p_i\left(\frac{y_1 - y_i}{\rho_i}\right)\rho_i \\ & & \sum_i p_i\left(\frac{z_1 - z_i}{\rho_i}\right)^2, & 0, 0, 0, & \sum_i p_i\left(\frac{z_1 - z_i}{\rho_i}\right)\rho_i \\ & & & & \text{(similar terms for station 2)} \\ & & & & \vdots \\ & \text{(symmetrical matrix of coefficients)} & & & \vdots \\ & & & & \sum_i p_i\rho_i^2 \end{bmatrix} \underbrace{\begin{bmatrix} dx_1 \\ dy_1 \\ dz_1 \\ dx_2 \\ dy_2 \\ dz_2 \\ \varepsilon \end{bmatrix}}_{\text{solution vector}} = \underbrace{\begin{bmatrix} \sum_i p_i\left(\frac{x_1 - x_i}{\rho_i}\right) d\rho_i \\ \sum_i p_i\left(\frac{y_1 - y_i}{\rho_i}\right) d\rho_i \\ \sum_i p_i\left(\frac{z_1 - z_i}{\rho_i}\right) d\rho_i \\ \text{(station 2)} \\ \vdots \\ \sum_i p_i\rho_i\, d\rho_i \end{bmatrix}}_{\text{residual vector}}$$

This matrix of coefficents will be very poorly conditioned, reflecting the indeterminacy of station navigation perpendicular to the Guier plane* (defined as that plane containing the station-to-satellite direction and the satellite velocity direction at the point of closest approach).

To improve the condition of our matrix, it is necessary to reduce the rank of the system in a manner that will minimally affect the interstation-range determination. Our technique is to rotate the coordinate system such that two of the unknowns (corresponding as closely as possible to the indeterminant parameters) can be dropped, thereby reducing the rank to five. This is done by adopting a local coordinate system with one station as the origin and the other station on the x axis. The direction from station 1 to the satellite at the point of closest approach, together with the x axis, defines the plane in which station 1 is navigated. The z axis is perpendicular to this plane and therefore dropped from the normal system. A similar plane is established for station 2, using the direction to the point of closest approach to station 2. The corresponding z axis for station 2 is also eliminated from the normal system. It will be noted that the two planes of navigation intersect at the interstation baseline.

The optimum station-to-satellite geometry is clearly that in which both stations lie in the orbital plane. In this case, we are navigating both stations in their coincident Guier planes. In all other cases, we are navigating in planes that merely approximate the Guier plane. However, except when the interstation baseline is nearly perpendicular to the orbital plane, the approximation is satisfactory.

---

*The Guier plane was first introduced by W. Guier in developing the basic analysis for doppler data supporting the Transit network. It has been carried over into all analyses of doppler data and has many additional advantages specific to doppler data, where a system parameter (the satellite oscillator correction) needs to be determined from each pass of data; in addition, certain environmental errors average out in that case. We have not investigated the extent to which those advantages can be utilized in this analysis, although intuitively we believe that, for example, in analyzing range data, refraction-model errors will be reduced.

Transformation to the local coordinate system is as follows:

$$\begin{bmatrix} X \\ Y \\ Z \end{bmatrix} = \left[\mathscr{R}\right] \begin{bmatrix} (x - x_1) \\ (y - y_1) \\ (z - z_1) \end{bmatrix} \quad ,$$

where $\mathscr{R}$ is defined as three rows of three vectors $\hat{R}_1$, $\hat{R}_2$, and $\hat{R}_3$:

$$\vec{R}_1 = (x_2 - x_1, y_2 - y_1, z_2 - z_1) \quad ,$$

$$\hat{R}_1 = \frac{\vec{R}_1}{|\vec{R}_1|} \quad ,$$

$$\vec{J}_{pca} = (x_{pca} - x_1, y_{pca} - y_1, z_{pca} - z_1) \quad ,$$

$$\vec{R}_3 = \hat{R}_1 \times \vec{J}_{pca} \quad ,$$

$$\hat{R}_3 = \frac{\vec{R}_3}{|\vec{R}_3|} \quad ,$$

$$\hat{R}_2 = \hat{R}_3 \times \hat{R}_1 \quad .$$

The orientation vector $\mathscr{R}$ for the transformation of station 2 and its observed satellites is similar except that the coordinates of the point of closest approach, x_{pca}, y_{pca}, and z_{pca}, refer to a different position and

$$\vec{J}_{pca} = (x_{pca} - x_2, y_{pca} - y_2, z_{pca} - z_2) \quad .$$

It can be seen that equation (2) is an adjustment performed by varying a scale parameter and the coordinates of the two station positions, each station constrained to a distinct plane. The two constraint planes intersect at the baseline, so the baseline length is unaffected. Satellite positions are not adjusted and must be taken <u>a priori</u>. Clearly, the results we obtain are functions of the assumed satellite positions, and care must be taken to use the best estimates possible.

For this analysis, we use the same precision differential-orbit-improvement program that we use in our gravity-field determination and our long-arc station-coordinate determination. One useful feature of this computer program is the capability of archiving on magnetic tape a large assemblage of data, including all adjusted satellite positions at the times of the observations.

The procedure, then, is to determine an orbit (typically spanning 10 days) from all available observations. When an orbit is optimized, it is no longer necessary to recompute the archive file, but only to access it in order to obtain a trajectory from best-fitting (in a global sense) estimates of satellite positions. The archive file is also a convenient place to keep observations, station coordinates corrected for tidal motion, pole position, sidereal time, and other auxiliary information.

Since the orbital routine operates in an inertial frame of reference, it is necessary to transform the satellite and station positions to a rotating (terrestrial) system according to the well-known relation:

$$\vec{x}_t = \begin{bmatrix} 1 & 0 & P_x \\ 0 & 1 & -P_y \\ -P_x & P_y & 1 \end{bmatrix} \begin{bmatrix} \cos\theta & \sin\theta & 0 \\ -\sin\theta & \cos\theta & 0 \\ 0 & 0 & 1 \end{bmatrix} \vec{x}_i \quad ,$$

where $\vec{x}_i$ is the inertial position, $\vec{x}_t$ is the terrestrial position, θ is the sidereal angle, and P_x and P_y are the pole-position angles in radians.

3. DATA ANALYSIS

The results reported here are based on the data available in mid-1977. Clearly, future data will be more comprehensive and the results more accurate. Furthermore, the data currently available were not taken for use with scalar translocation. In this section, we discuss the data available, give an example of a baseline determination, and review the translocation results to date.

The locations of laser stations used in this analysis are plotted on a map in Figure 3. Our analysis included data from the retroreflector-equipped satellites listed in Table 1. Unfortunately, the basic assumption — that two (or more) stations observe the same part of an orbital arc — limits the number of events to be analyzed. For stations with wide geographical distribution, a high satellite such as Lageos is necessary, but Lageos has been in orbit only for about 1 year. While geographically close stations can use lower satellites, few of the clusters of stations in western Europe and western United States operated for any extended periods of time. The data available to us for this program have accuracies as outlined in Table 1.

Some caveats are in order regarding the data in Table 1. First, the 1967-1968 data (provided by the Centre National d'Etudes Spatiales) were taken with first-generation laser stations. The 1- to 2-m noise should be no limit on the analysis. It was argued above that the bias, probably 1 to 2 m, should cancel; however, epoch timing was certainly no better than 1 msec and probably worse, which immediately places an accuracy limit of 5 to 10 m for each event. Second, the 1974 San Diego—Quincy baseline is almost north—south, and the laser data (provided by the National Aeronautics and Space Administration's Goddard Space Flight Center) were taken on the BE-C satellite. With an inclination of 39° (approximately the latitude of the northern station, Quincy), BE-C's tracks passed normal to the baseline, resulting in a poor overall geometry. The baseline from San Diego to Mt. Hopkins was east—west, which is favorable, but the data from Mt. Hopkins were only of 1- to 2-m accuracy. In 1974, the laser at Mt. Hopkins operated with a low repetition rate, which limited the data available. Furthermore, the 1976 Lageos data from Brazil, Peru, and

Mt. Hopkins were of 1 to 2 m in quality. Finally, there were only eight successful simultaneous passes from San Diego to Bear Lake.

From this mixture of data, we present detailed results from the San Diego—Mt. Hopkins baseline. The 1974 data on BE-C were run in 7-day arcs using all the available laser data, a 24th-degree-and-order gravity field, and initial coordinates derived from the analysis of laser tracking data on nine satellites. The laser data, being of unequal number for each station, were edited to obtain approximately a maximum of 150 points evenly distributed throughout each satellite pass. We used simultaneous events in which any overlap in the observed part of the orbit occurred; therefore, most of each observed arc was not common to both stations. From the orbital residuals (rms = 5 m), each station was navigated in its special coordinate system, as described above, by using a least-squares estimator and assigning uncertainties of 10 cm to the San Diego data and 1 m to Mt. Hopkins.

Twenty simultaneous events were obtained on BE-C from this 2-month period; results of the individual baselines determined are given in Table 2. Some long-wavelength structure (compared to the pass length) remains in the residuals — i.e., the orbital motion yet to be modeled — indicating that our assumption about the shape of the trajectory may not be completely true. However, this structure, when present, does not seem to limit the baseline accuracy. Since this method was first developed, improvements in both gravity-field models and orbital theory have noticeably reduced the amount of structure in short-arc analyses. Although such structure increases the formal uncertainty of a baseline determination, it does not, in the mean, change the value of the averaged baseline. Therefore, as general orbit-computation capabilities improve, we can expect individual baselines to be more accurately determined, thereby either increasing the accuracy of the averaged baseline or reducing the number of individual determinations necessary to obtain a given accuracy.

Each solution was iterated to delete bad observations. Using the computed uncertainty as a weight, we obtained the mean of 19 events (one was deleted); the results are summarized in Table 3.

The same analysis procedure was done on Lageos data taken in 1976. The main difference here is that the Lageos satellite is in a much higher altitude than BE-C and has a significantly smaller area-to-mass ratio. Therefore, both gravitational and nongravitational perturbations are smaller and the uncertainties in these perturbations are smaller still. The overall orbital fit for Lageos is considerably better, and the amount of structure in the residuals is very small. The residuals for one arc of Lageos data are shown in Figure 4, while the results of the 14 baselines determined on this satellite are given in Table 4. In the figure, the data from both stations are on the same time base, but the meter scale has been adjusted to reflect the difference in noise levels. The weighted mean of these results is given in Table 5.

Combining the 33 San Diego—Mt. Hopkins baselines, we computed a single weighted mean, shown in Table 6.

Finally, Table 7 presents the results of a scalar transformation analysis performed from the data in Table 1.

CONCLUSIONS

A. Scalar translocation can provide baseline determinations independent of GM and a global scale based on the light second. The accuracy is currently better than 1 m, and, aside from data accuracy, there seems to be no limitation to obtaining results with an accuracy better than 10 cm. This accuracy is independent of baseline length.

B. Both high and low satellites can be used with equal success.

C. Scalar translocation baselines provide another independent data type that can be combined with other data to obtain a global reference system.

D. Continued acquisition of laser data and continued improvements in data accuracy and in orbit-computation capabilities will enable baseline determinations to be made with centimeter accuracy.

5. ACKNOWLEDGMENT

This work was supported in part by Grant NSG-5148 from the National Aeronautics and Space Administration.

6. REFERENCES

Aardoom, L., Girnius, A., and Veis, G., 1967, Determination of the absolute space directions between Baker-Nunn camera stations. In The Use of Artificial Satellites for Geodesy, ed. by G. Veis, National Tech. Univ., Athens, vol. II, pp. 315-344.

Anderle, R. J., 1974, Transformation of terrestrial survey data to doppler satellite datum. Journ. Geophys. Res., vol. 79, pp. 5319-5331.

Blaha, G., 1971, Investigation of critical configurations for fundamental range networks. Ohio State Univ. Dept. Geodetic Sci. Rep. No. 150, 274 pp.

Blaha, G., 1972, Critical configurations of fundamental range networks. In The Use of Artificial Satellites for Geodesy, ed. by S. W. Henriksen, A. Mancini, and B. H. Chovitz, Amer. Geophys. Union Monograph No. 15, pp. 1-8.

Brown, D. C., 1976, Doppler positioning by the short arc method. Presented at the International Geodetic Symposium, Satellite Doppler Positioning, Las Cruces, New Mexico, October.

Gaposchkin, E. M., editor, 1973, 1973 Smithsonian Standard Earth (III). Smithsonian Astrophys. Obs. Spec. Rep. No. 353, 388 pp.

Gaposchkin, E. M., and Lambeck, K., 1970, 1969 Smithsonian Standard Earth (II). Smithsonian Astrophys. Obs. Spec. Rep. No. 315, 93 pp.

Lundquist, C. A., and Veis, G., editors, 1966, Geodetic Parameters for a 1966 Smithsonian Institution Standard Earth. Smithsonian Astrophys. Obs. Spec. Rep. No. 200, 3 vols., 686 pp.

Melchior, P., publisher, 1975, Comptes Rendus de la XVIe Assemblée Générale de l'U.G.G.I., I.U.G.G. Publ. Office, Paris.

Schmid, H. H., 1974, Worldwide geometric satellite triangulation. Journ. Geophys. Res., vol. 79, pp. 5349-5376.

Smith, D. E., Lerch, F. J., Marsh, J. G., Wagner, C. A., Kolenkiewicz, R., and Kahn, M. A., 1976, Contribution to the National Geodetic Satellite Program by Goddard Space Flight Center. Journ. Geophys. Res., vol. 81, pp. 1006-1026.

Strange, W., Hothem, L. D., White, M., 1975, Results of satellite positioning in the United States. Presented at the 1975 Spring Annual Meeting of the American Geophysical Union, Washington, D.C., June.

Veis, G., 1967, Results from geometric methods. In Space Research VII, ed. by R. L. Smith-Rose, S. A. Bowhill, and J. W. King, North-Holland Publ. Co., Amsterdam, pp. 778-782.

Table 1. Translocation data summary.

Year	Stations	Satellites	Duration	Data accuracy
1967	France; Greece	Geos 1, D1C, D1D	2 months	2 m
1968	France; Spain	Geos 1 and 2, D1C, D1D	2 months	2 m
1974	Mt. Hopkins, Ariz.; San Diego, Calif.; Quincy, Calif.	BE-C	2 months	10 cm to 2 m
1976	Bermuda; Grand Turk; GSFC, Maryland; Patrick AFB, Calif.	Geos 3, Starlette, BE-C	on-going	10 cm
1976	Brazil; Peru; Mt. Hopkins; GSFC	Lageos	2 months	10 cm to 1 m
1976	Brazil; Peru; Mt. Hopkins; San Diego; Quincy; Bear Lake, Utah	Lageos	2 months	10 cm to 1 m

Table 2. Individual baselines determined from 1974 BE-C data between Mt. Hopkins and San Diego.

MJD	San Diego Max elev.	San Diego Points	Mt. Hopkins Max elev.	Mt. Hopkins Points	Overlap time (min)	Condition number	Scale (ppm)	Baseline (m)
42336	45°	62	42°	26	6.1	3.1×10^3	-4.7	571554.547 ± 0.6544
42336	74	54	63	27	9.5	6.2×10^2	0.7	571548.495 ± 0.8048
42337	51	80	53	37	10.5	5.0×10^2	3.1	571552.680 ± 0.5790
42337	86	111	75	39	12.0	4.9×10^2	0.8	571548.612 ± 0.9168
42345	44	7	43	22	3.4	3.9×10^3	-2.1	571554.129 ± 0.6377
42345	68	53	75	31	7.3	5.0×10^2	0.0	571552.872 ± 0.7775
42345	50	31	41	31	7.1	1.3×10^3	-5.1	571551.490 ± 0.6920
42388	68	53	79	9	7.2	1.7×10^3	0.0	571561.104 ± 13.77
42388	56	56	47	10	5.2	3.3×10^3	-2.2	571552.967 ± 10.56
42390	46	36	63	13	3.3	2.4×10^3	1.9	571563.591 ± 1.124
42390	71	51	58	18	6.9	9.4×10^2	1.5	571558.446 ± 3.942
42391	38	51	52	30	10.8	7.7×10^2	1.1	571560.289 ± 2.589
42391	81	55	70	38	11.1	2.6×10^2	2.2	571557.493 ± 3.293
42391	47	53	42	33	9.2	5.2×10^2	-1.2	571552.937 ± 1.751
42391	51	42	53	20	1.1	2.3×10^3	5.1	571553.692 ± 0.7093
42392	87	49	74	41	10.2	2.5×10^2	2.2	571559.756 ± 2.276
42392	50	63	44	26	7.7	9.6×10^2	-0.4	571554.976 ± 2.267
42392	48	40	49	24	5.1	4.3×10^3	2.5	571552.393 ± 0.7034
42394	60	55	50	32	10.1	3.9×10^2	-0.5	571554.632 ± 4.430
42395	52	52	69	23	5.7	1.6×10^3	1.2	571558.548 ± 5.258

Table 3. Results of 1974 San Diego — Mt. Hopkins baseline.

Baseline	571552.685 ± 0.510 m
rms	2.16 m
σ_0	2.19

Table 4. Individual baselines from 1976 Lageos data between Mt. Hopkins and San Diego.

MJD	San Diego Max elev.	San Diego Points	Mt. Hopkins Max elev.	Mt. Hopkins Points	Overlap time (min)	Condition number	Scale (ppm)	Baseline (m)
43077	63°	49	57°	69	17.2	2.0×10^3	-1.0	571552.612 ± 1.392
43080	61	77	66	51	34.6	2.3×10^3	-1.3	571556.037 ± 1.123
43081	70	76	80	65	41.8	6.5×10^2	-1.6	571556.198 ± 0.4878
43082	48	81	47	68	11.8	9.2×10^3	-1.6	571555.416 ± 1.745
43086	79	182	89	142	34.6	9.5×10^2	-1.5	571556.111 ± 0.3166
43087	31	23	61	119	3.7	3.7×10^3	-0.5	571552.249 ± 1.659
43090	56	168	49	55	29.3	3.6×10^3	-0.1	571549.287 ± 0.5390
43092	25	174	25	11	8.1	8.3×10^4	0.8	571554.450 ± 2.202
43098	52	25	47	66	1.6	2.2×10^4	-0.6	571554.349 ± 2.296
43101	42	173	46	136	31.6	1.1×10^3	-0.1	571554.365 ± 0.3272
43104	37	184	40	58	11.0	2.7×10^4	-0.1	571553.893 ± 0.9981
43106	49	166	54	68	22.4	2.7×10^3	-0.6	571554.150 ± 0.4635
43106	42	102	47	78	7.3	4.4×10^4	0.1	571549.649 ± 1.240
43107	74	155	78	91	32.8	1.7×10^3	-1.4	571555.108 ± 0.5900

Table 5. Results of 1976 San Diego — Mt. Hopkins baseline.

Baseline	571554.582 ± 1.14 m
rms	2.05 m
σ_0	3.40

Table 6. Combined results for San Diego – Mt. Hopkins baseline.

Baseline	571553.947 ± 0.401 m
rms	2.27 m
σ_0	3.01

Table 7. Baseline determinations.

Station pair	Location	Distance (m)	rms (m)	Number of observations
7061 — 7921	San Diego — Mt. Hopkins	571553.947 ± 0.401	2.271	33
7907 — 7921	Peru — Mt. Hopkins	6471755.860 ± 0.808	3.790	23
7907 — 7929	Peru — Brazil	4055910.289 ± 0.833	3.228	16
7061 — 7080	San Diego — Quincy	896271.494 ± 0.993	4.439	21
7063 — 7921	GSFC — Mt. Hopkins	3147781.344 ± 0.619	2.052	12
7921 — 7082	Mt. Hopkins — Bear Lake	1137306.990 ± 0.758	2.004	8
7061 — 7082	San Diego — Bear Lake	1140020.309 ± 0.711	2.012	9

FIGURE CAPTIONS

Figure 1. Illustration of the effect of an error in GM.

Figure 2. Coordinate system used in the translocation analysis.

Figure 3. Illustration of the network of baselines obtained from the method of translocation.

Figure 4. Plot of range residuals versus time for Lageos after adjustment by the translocation method. The baseline is between San Diego and Mt. Hopkins.

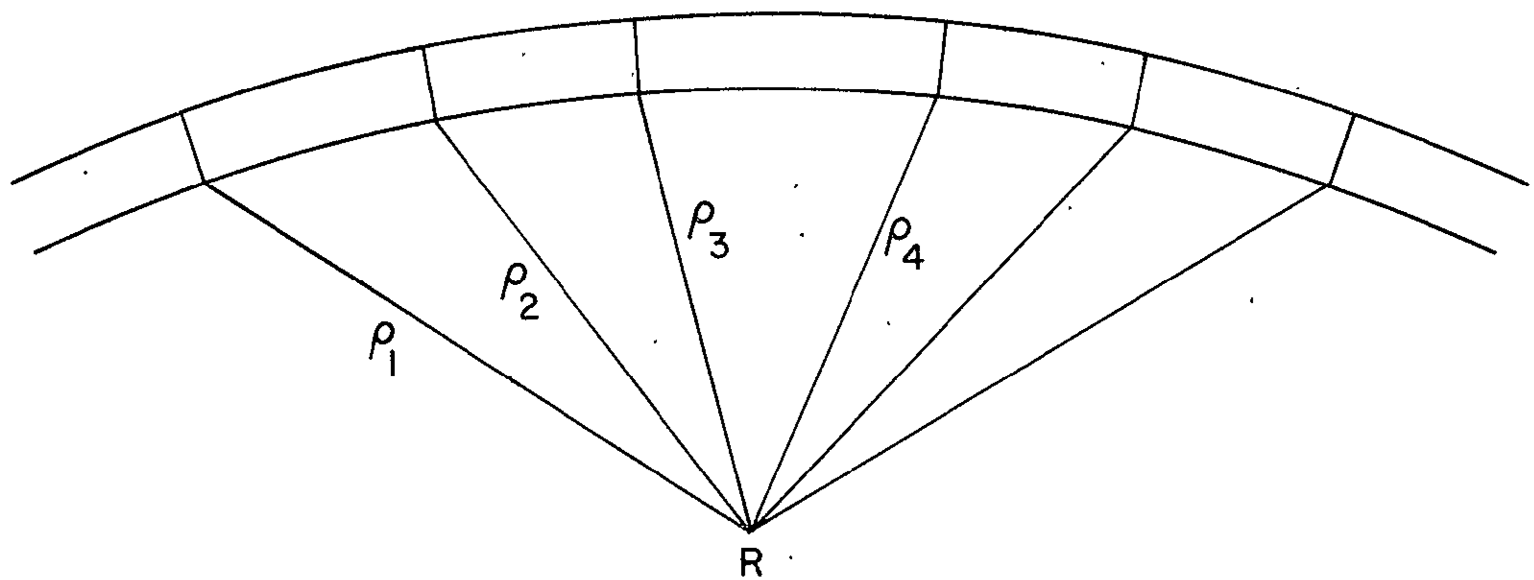

Figure 1

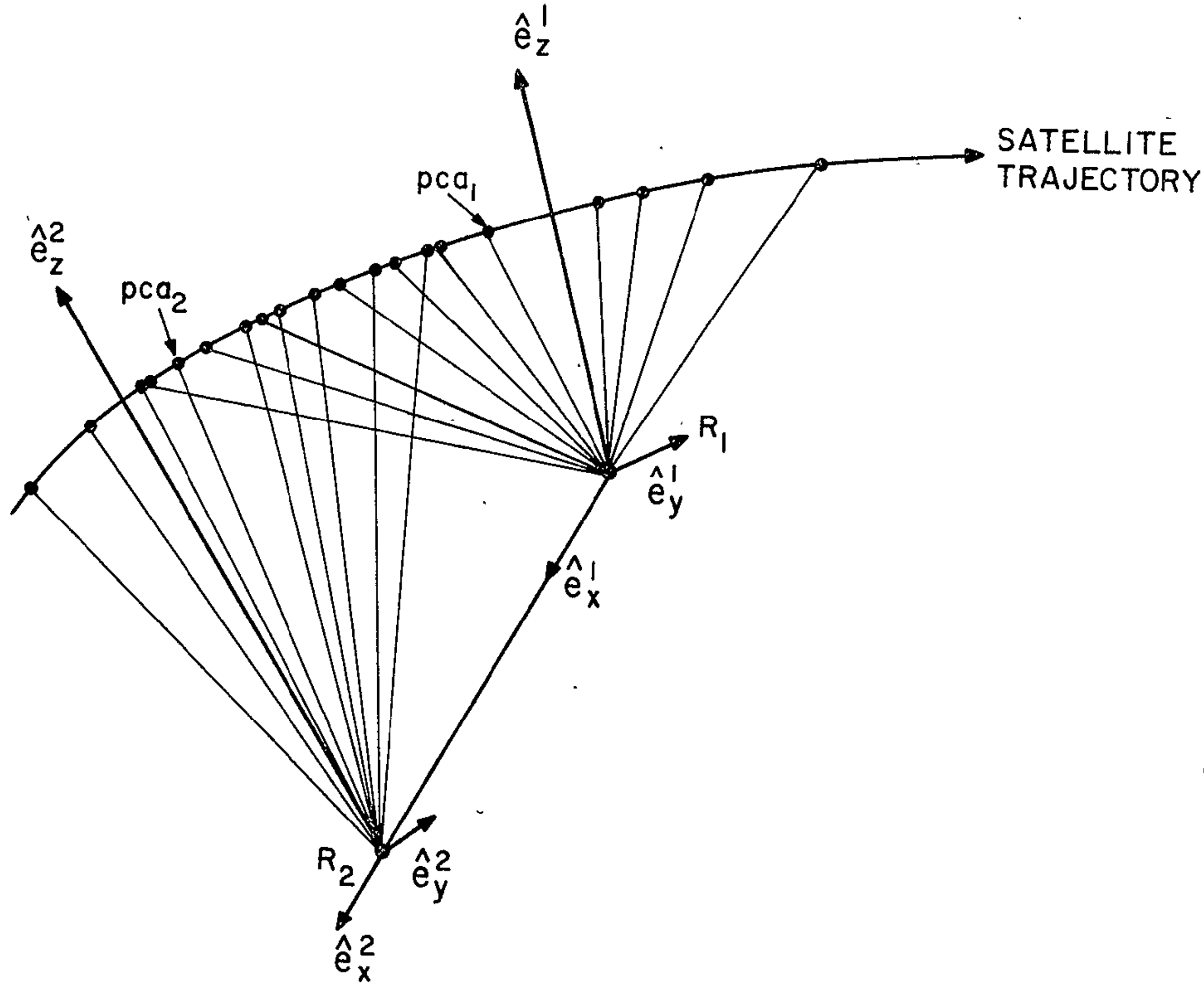
$\hat{e}_z^1$
SATELLITE TRAJECTORY
pca_1
$\hat{e}_z^2$
pca_2
R_1
$\hat{e}_y^1$
$\hat{e}_x^1$
R_2
$\hat{e}_y^2$
$\hat{e}_x^2$

Figure 2

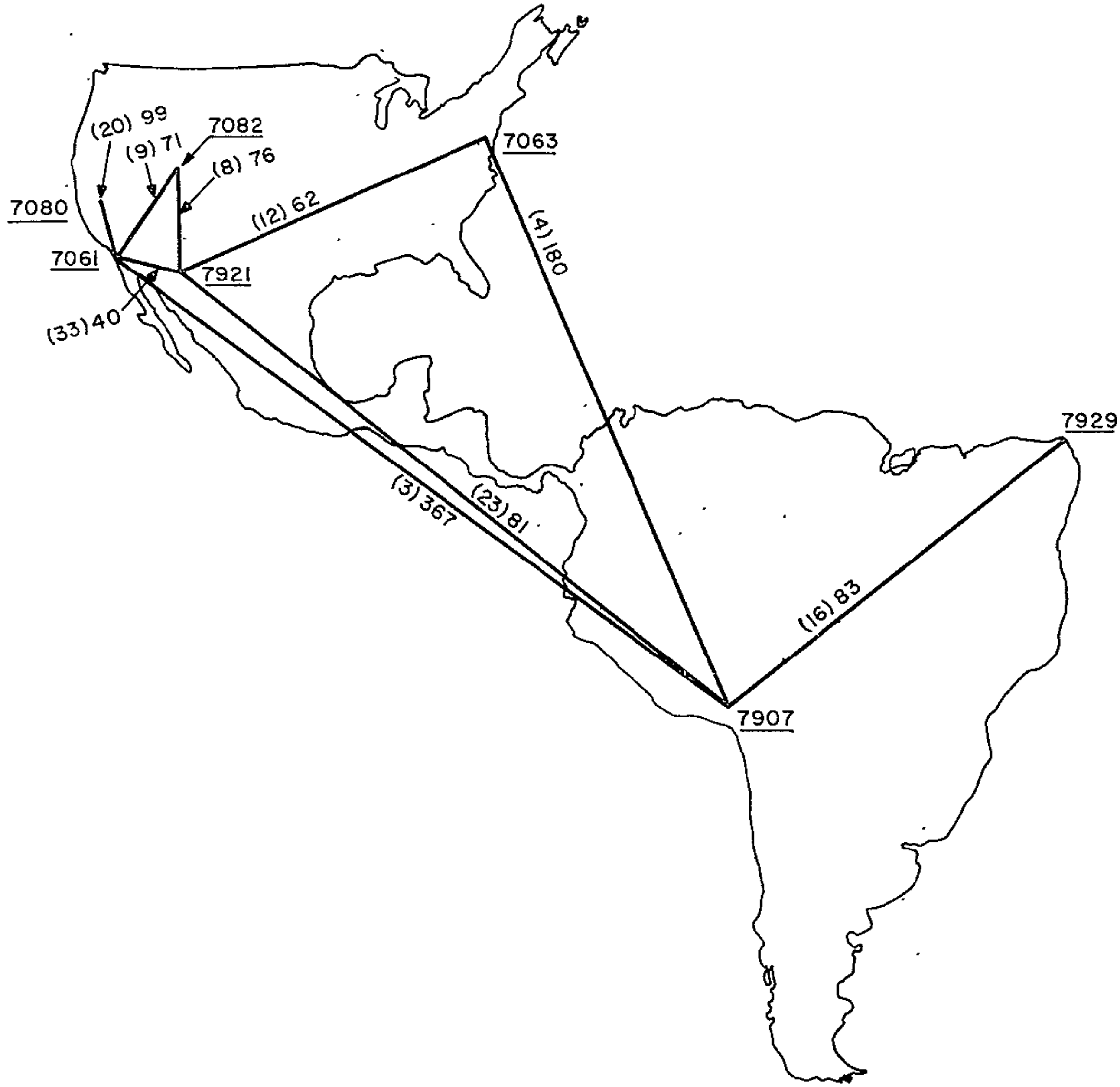

(20) 99
(9) 71
7082
(8) 76
7063
7080
(12) 62
(4) 180
7061
7921
(33) 40
7929
(3) 367
(23) 81
(16) 83
7907

Figure 3

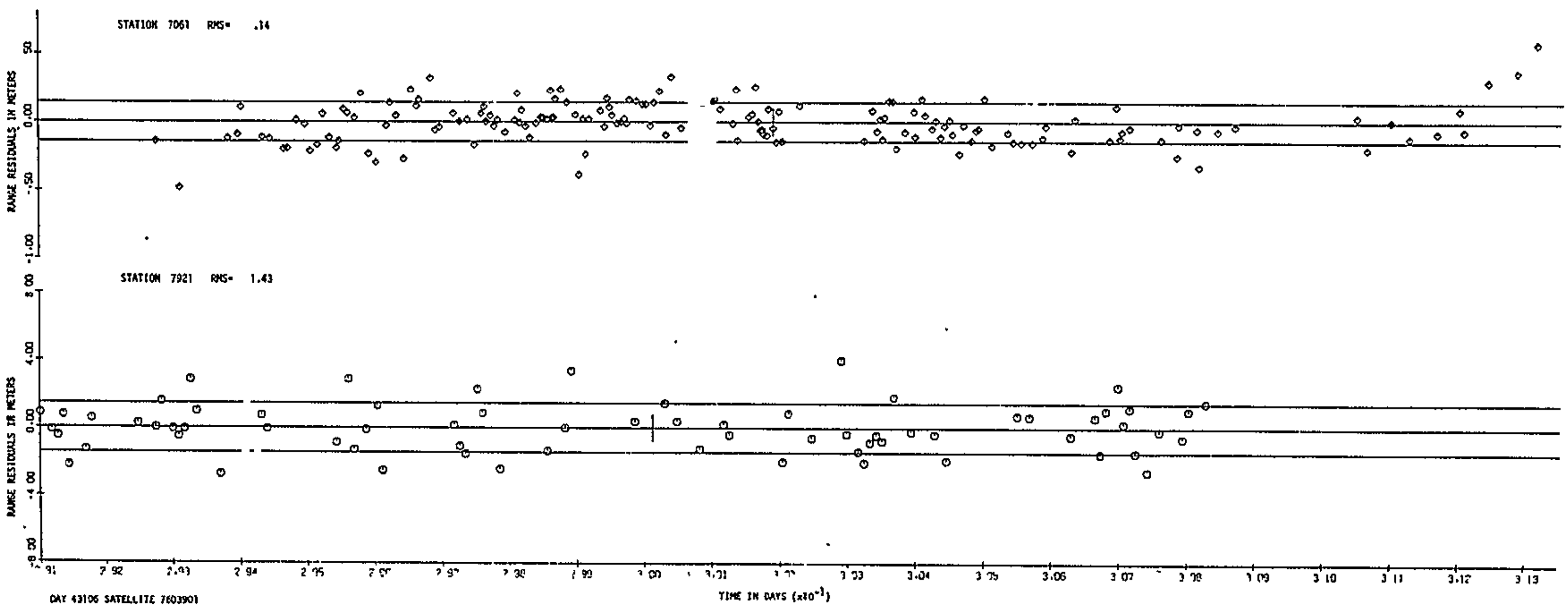
STATION 7061 RMS= .14
RANGE RESIDUALS IN METERS
STATION 7921 RMS= 1.43
RANGE RESIDUALS IN METERS
DAY 43106 SATELLITE 7603901
TIME IN DAYS (x10⁻¹)

Figure 4